Dynamos on stream surfaces of a highly conducting fluid

Andrew D. Gilbert and Yannick Ponty,
School of Mathematical Sciences,
University of Exeter,
Exeter EX4 4QE, U.K.

Abstract

This paper discusses dynamo action in generalisations of the Ponomarenko dynamo at large magnetic Reynolds number. The original Ponomarenko dynamo consists of a spiralling flow in which the stream surfaces are concentric cylinders of circular cross section, and the flow depends only on distance from the axis in cylindrical polar coordinates.

In this study, the stream surfaces are allowed to be cylinders of arbitrary cross section, and the flow is only required to be independent of the coordinate along the cylinder axes. For smooth flows alpha and eddy diffusion effects are identified, in terms of the geometry of the stream surfaces, and asymptotic formulae for growth rates in the limit of large magnetic Reynolds number are obtained. Numerical support for these results is presented using direct simulation of dynamo action in selected flows at high conductivity. Finally the case is considered when in spherical polar coordinates the flow is independent of the azimuthal coordinate and the stream surfaces, which are tori, have arbitrary cross sections.

1. Introduction

The Ponomarenko dynamo is perhaps the simplest of all dynamos. In cylindrical polar coordinates, the flow field depends only on the distance r from the axis of the coordinate system. In the original paper of Ponomarenko (1973) the flow has a piecewise constant axial velocity $W(r)$ and angular velocity $\Omega(r)$. Inside a cylinder of a given radius the fluid is in solid body motion, of axial translation and uniform rotation, while outside the fluid is at rest. All the differential rotation, leading to the stretching of magnetic field, is concentrated at the cylinder boundary where the flow is discontinuous. This, together with the effect of diffusion in cylindrical geometry, allows dynamo action to take place. Ponomarenko dynamos have been discussed as models of magnetic field generation in galactic jets (Shukurov & Sokoloff 1993), and form the basis of experiments to realise a laboratory dynamo (Gailitis *et al.* 1987, 1999, Gailitis 1993). We also note the close relation between the Ponomarenko geometry and the earlier exact dynamo models of Lortz (1968).

The simplicity of Ponomarenko's original model allows the dispersion relation to be written down analytically in terms of Bessel functions, and growth rates can be obtained numerically for critical values of the magnetic Reynolds number R (Gailitis & Freiberg 1980) and asymptotically for large R (Roberts 1987). In fact at large R the dynamo is technically a fast dynamo, the maximum growth rate being of the order of the turn-over time scale, independent of R as $R \to \infty$ (Gilbert 1988). This fast behaviour is however

intimately connected with the discontinuity of the flow, which introduces a zero length scale into the problem, and is not typical of smooth chaotic fast dynamos (see Childress & Gilbert 1995, section 5.4.1).

The model of Ponomarenko may be extended in many ways. The basic mechanism is very general: differential rotation generates azimuthal and axial field from radial field, while diffusion in curved geometry closes the dynamo loop by regenerating radial field from azimuthal field. The simplest extension is to allow the flow field to be continuous, say a smooth function of radius, while retaining cylindrical stream surfaces. This is studied numerically by Solovyev (1985, 1987) and asymptotically by Gilbert (1988) and Ruzmaikin, Sokoloff & Shukurov (1988). The basic mechanism remains the same but the scalings change, because the differential rotation is now distributed in radius. The fastest growing modes have growth rates $p = O(R^{-1/3})$ and wave numbers of order $R^{1/3}$. The dynamo is thus slow; see Basu (1997) for a general result along these lines.

In the limit of large R the magnetic modes localise on stream surfaces given by a resonance condition, that the shear at the stream surface should be aligned with the magnetic field lines. In fact on some stream surfaces dynamo action is not possible at high R. To obtain amplification on a given stream surface at large R, it is necessary that the fluid flow in its neighbourhood should obey a purely geometrical condition, that the pitch of the shear should not change too rapidly with radius, namely

$$\frac{r}{4}\left|\frac{d}{dr}\log\left|\frac{\Omega'(r)}{W'(r)}\right|\right| < 1 \tag{1.1}$$

(Gilbert 1988, Ruzmaikin *et al.* 1988).

The aim of the present paper is to generalise Ponomarenko dynamos further. We shall stay within the class of smooth flows, but broaden the range of possible geometries. This paper considers three obvious ways in which this can be done. First we can allow the stream surfaces to become cylinders of arbitrary cross section. Secondly we can allow the axial z-velocity to be an arbitrary smooth function of x and y, rather than being constant on stream surfaces. These first two generalisations allow us to study dynamo action on stream surfaces in general flows independent of the z-coordinate. Finally we can replace the Cartesian geometry by a spherical polar geometry with coordinates (r, θ, ϕ), in which the flow is independent of the azimuthal ϕ-direction.

It is clear that in these generalisations the basic Ponomarenko mechanism must still be present and lead to amplification under certain conditions. We shall consider the astrophysically important limit of large magnetic Reynolds number, in which the magnetic field becomes localised on stream surfaces and an analytical approach based on this becomes possible. For low R, the field is more diffuse and normally one must resort to computer simulation to obtain growth rates. Nevertheless high-R asymptotic results are a useful guide to the generation of field in flows even when the actual values of R may be quite modest; for example high-R asymptotics may give accurate critical values of R for dynamo instability (see section 5 below, and figure 9). We shall obtain asymptotic formulae for growth rates at large R, and to generalise the dynamo criterion (1.1) above. We note that the formulae we obtain will inevitably involve integrals around stream surfaces that capture the geometrical complications of the flow fields, and that these must usually be evaluated numerically in all except the simplest fluid flows.

The more general geometry we consider is relevant to modelling and numerical simulation of dynamos. The present paper is motivated by our observations of dynamo action in convective rolls with persistent axial flows, obtained in simulations of rotating sheared convection in a plane layer (Ponty, Gilbert & Soward 2000). In certain regimes dynamo action occurs by the Ponomarenko mechanism and visualisation of the magnetic field shows clearly the correct form of spiralling tubes of field localised on a stream surface. However in these quite complicated systems there is no reason why the stream surfaces should be cylindrical, nor why the velocity along the rolls should be constant on stream surfaces.

Another example is given by Plunian, Marty & Alemany (1999) who model flows in the cooling systems of nuclear reactors using a cellular flow. Their numerical study of kinematic dynamo action reveals growth through the Ponomarenko mechanism, and through competing 'Roberts modes' in which magnetic fields are localised on the separatrices between neighbouring cells (see Roberts 1970, Childress 1979, Soward 1987). Other flows with a similar stream surface topology to the smooth Ponomarenko dynamo, but now in spherical polar coordinates, are the roll dynamos of Dudley & James (1989) (see their equations (24–26)). These have toroidal stream surfaces on which the Ponomarenko dynamo mechanism could occur, although we are not aware of any studies at large R.

All the classes of flows we consider fall within the study of Soward (1990), whose very general framework of hybrid Eulerian–Lagrangian coordinates allows magnetic field generation localised on stream surfaces, together with fluctuating flows that go to zero with increasing magnetic Reynolds number (see Braginsky 1964a,b). Although this framework certainly includes all the models we study in this paper, Soward (1990) does not derive formulae for growth rates, except in special cases, nor does he generalise the criterion (1.1). Our aim is to obtain explicit formulae which may be used and tested numerically. We find it easiest to set up a coordinate system that is immediately adapted to the classes of Ponomarenko dynamos we consider and to obtaining asymptotic growth rates numerically (see section 5.2), rather than adapt the very general framework of Soward (1990).

The paper is organised as follows. In section 2 we consider the first of our models. Working in Cartesian coordinates the flow is given by $\mathbf{u} = (-\psi_y, \psi_x, W)$ where $\psi(x, y)$ is the stream function and the vertical flow W is constant on stream surfaces. We set up a coordinate system based on the shape of the stream surfaces, and rewrite the induction equation in this system. Our choice of coordinates is aimed to simplify the advection and stretching of the magnetic field as far as possible, and we can then approximate the processes of diffusion so as to pick up only important terms in the limit of large R. When this is done we obtain a dynamo driven by an alpha effect, which we call α_m, that immediately generalises the results of Gilbert (1988) and Ruzmaikin *et al.* (1988). We note that an example studied by Soward (1990) falls into the family of flows we discuss in section 2. In section 5 of Soward (1990) an integrable ABC flow with $A = 0$ and $B \neq C$ is considered, which corresponds to $\psi = -B\cos x - C\sin y$ and $W(\psi) = -\psi$ in our notation. Soward finds dynamo action by the Ponomarenko mechanism, obtains explicit growth rates and determines the regions of the flow in which dynamo action can occur.

In section 3 we generalise the model of section 2 by allowing the vertical flow W to have an arbitary dependence on x and y, no longer being constrained to be constant on stream surfaces. This complicates our coordinate system and introduces a new alpha effect,

α_k. Section 4 develops a purely analytical example to illustrate the results of sections 2 and 3. We assume that the flow has elliptical stream lines and determine α_m and α_k in terms of the flow parameters. We test the results of sections 2 and 3 numerically, using large-scale simulations of kinematic dynamo action in a plane layer, in section 5.

We extend our earlier results to the case when the flow is independent of azimuthal angle in spherical polar coordinates in section 6 (see also the discussion in section 6 of Soward 1990). The stream surfaces are then tori of arbitrary cross section. Although the curved geometry complicates matters, the calculations very much parallel the case for Cartesian coordinates, and again there are two alpha effects that may be isolated. Finally section 7 offers some discussion.

2. Cartesian geometry with vertical velocity $W(\psi)$

We consider the dimensionless induction equation,

$$\partial_t \mathbf{b} + \mathbf{u}\cdot\nabla\mathbf{b} - \mathbf{b}\cdot\nabla\mathbf{u} = \varepsilon\nabla^2\mathbf{b}, \qquad \nabla\cdot\mathbf{b} = \nabla\cdot\mathbf{u} = 0, \tag{2.1a,b}$$

asymptotically in the limit $\varepsilon \to 0$, which corresponds to the limit of large magnetic Reynolds number $R = \varepsilon^{-1}$. We use Cartesian coordinates (x, y, z) with corresponding unit vectors $\{\hat{\mathbf{x}}, \hat{\mathbf{y}}, \hat{\mathbf{z}}\}$. Consider a flow independent of the vertical z-direction, taking the form

$$\mathbf{u} = \mathbf{u}_H(x, y) + W(x, y)\,\hat{\mathbf{z}}; \tag{2.2}$$

the horizontal part of the velocity $\mathbf{u}_H$ is defined using a stream function $\psi(x, y)$,

$$\mathbf{u}_H = -\partial_y\psi\,\hat{\mathbf{x}} + \partial_x\psi\,\hat{\mathbf{y}} = \hat{\mathbf{z}}\times\nabla\psi = -\nabla\times(\psi\hat{\mathbf{z}}). \tag{2.3}$$

In this section we restrict W to the case when $W = W(\psi)$; the general case is considered in section 3. This condition that the vertical velocity is uniform on each stream surface is useful as it simplifies the advection operator d_t below, and is a property satisfied by many well-known kinematic dynamo models (e.g., Roberts 1970).

2.1. Coordinate system

To begin with we will ignore the z-direction and z-component W of velocity, and consider motion under the stream function ψ in the (x, y)-plane only. We set up a new coordinate system (reminiscent of action–angle variables) adapted to the stream line topology and to the differential rotation in the flow (see Rhines & Young 1983, Bassom & Gilbert 2000). We use the stream function ψ as one coordinate. On a given stream line an advected fluid element has period $T(\psi)$. The element travels a distance ds in time $dt = ds/q$ with $q \equiv |\mathbf{u}_H|$. We assume that q is nowhere zero on the stream line, so that $\mathbf{u}_H$ has no stagnation points, and define an angle coordinate ϑ by

$$d\vartheta = \frac{2\pi}{T(\psi)}\,dt \equiv \Omega(\psi)\,dt = \Omega(\psi)\,\frac{ds}{q} \qquad (q \equiv |\mathbf{u}_H|,\ \Omega(\psi) \equiv 2\pi/T(\psi)), \tag{2.4}$$

with a suitable choice of origin $\vartheta = 0$. Clearly ϑ changes by 2π during one complete traversal of the stream line and $\Omega(\psi)$ is an angular velocity, constant on stream lines. We do this for all stream lines to define ϑ as a coordinate and then use (ψ, ϑ) coordinates in place of (x, y)-coordinates (see figure 1).

If we now reinstate the z-coordinate and vertical velocity $W(\psi)$, a fluid element passively advected in the fluid flow has coordinates (ψ, ϑ, z) which obey

$$\dot{\psi} = 0, \quad \dot{\vartheta} = \Omega(\psi), \quad \dot{z} = W(\psi). \tag{2.5}$$

Correspondingly the advection operator becomes

$$d_t \equiv \partial_t + \mathbf{u} \cdot \nabla = \partial_t + \Omega(\psi)\partial_\vartheta + W(\psi)\partial_z. \tag{2.6}$$

Using the Cauchy solution we may obtain the motion of field vectors in the case of zero diffusion, $\varepsilon = 0$ in (2.1). Consider a magnetic field vector frozen in the flow, represented by increments $(\delta\psi, \delta\vartheta, \delta z)$ in the coordinates, proportional to the components

$$b_\psi \equiv \mathbf{b} \cdot \nabla\psi, \quad b_\vartheta \equiv \mathbf{b} \cdot \nabla\vartheta, \quad b_z \equiv \mathbf{b} \cdot \hat{\mathbf{z}}; \tag{2.7}$$

plainly these components will obey

$$d_t b_\psi = 0, \quad d_t b_\vartheta = \Omega'(\psi) b_\psi, \quad d_t b_z = W'(\psi) b_\psi \qquad (\varepsilon = 0), \tag{2.8}$$

from differentiating (2.5).

In equation (2.7) we are using the basis $\{\nabla\psi, \nabla\vartheta, \hat{\mathbf{z}}\}$ to measure magnetic field components. These vectors are linearly independent (as $q \neq 0$) and form a right-handed set. We denote the reciprocal basis by $\{\mathbf{e}_\psi, \mathbf{e}_\vartheta, \hat{\mathbf{z}}\}$, as shown in figure 2. To relate these bases consider a small element of fluid determined by small changes $\delta\psi$ and $\delta\vartheta$ in the coordinates. This element is also spanned by the vectors $\delta\psi\,\mathbf{e}_\psi$ and $\delta\vartheta\,\mathbf{e}_\vartheta$, and so has area $(\mathbf{e}_\psi \times \mathbf{e}_\vartheta \cdot \hat{\mathbf{z}})\,\delta\psi\,\delta\vartheta$. In a short time δt, ϑ changes by an amount $\Omega(\psi)\,\delta t$, corresponding to the passage of an area $\Omega(\psi)(\mathbf{e}_\psi \times \mathbf{e}_\vartheta \cdot \hat{\mathbf{z}})\,\delta\psi\,\delta t$ of fluid between the stream lines ψ and $\psi + \delta\psi$. However this must be equal to $\delta\psi\,\delta t$ by the property of the stream function that $\delta\psi$ is the flux of fluid between two stream lines given by ψ and $\psi + \delta\psi$. Hence

$$\mathbf{e}_\psi \times \mathbf{e}_\vartheta \cdot \hat{\mathbf{z}} = (\nabla\psi \times \nabla\vartheta \cdot \hat{\mathbf{z}})^{-1} = \Omega(\psi)^{-1}. \tag{2.9}$$

Thus we obtain the reciprocal basis vectors explicitly as

$$\mathbf{e}_\psi = \Omega(\psi)^{-1}\nabla\vartheta \times \hat{\mathbf{z}}, \quad \mathbf{e}_\vartheta = \Omega(\psi)^{-1}\hat{\mathbf{z}} \times \nabla\psi = \Omega(\psi)^{-1}\mathbf{u}_H. \tag{2.10a,b}$$

Using the properties of reciprocal bases, from (2.7) the magnetic field may be written as $\mathbf{b} = b_\psi \mathbf{e}_\psi + b_\vartheta \mathbf{e}_\vartheta + b_z \hat{\mathbf{z}}$.

2.2. Diffusion

The calculations in the previous subsection using the Cauchy solution for $\varepsilon = 0$ simplify the left-hand side of the induction equation (2.1a). For general ε, this now becomes

$$d_t b_\psi = \varepsilon \nabla\psi \cdot \nabla^2 \mathbf{b}, \tag{2.11a}$$

$$d_t b_\vartheta - \Omega'(\psi) b_\psi = \varepsilon \nabla\vartheta \cdot \nabla^2 \mathbf{b}, \tag{2.11b}$$

$$d_t b_z - W'(\psi) b_\psi = \varepsilon \hat{\mathbf{z}} \cdot \nabla^2 \mathbf{b} \tag{2.11c}$$

from (2.8). Note that there is a source term on the left-hand side of the second and third of these equations whereby b_ϑ and b_z fields are generated by differential rotation from the b_ψ field: this is an 'omega effect'. However to complete the dynamo 'loop' we require some means of regenerating b_ψ field and this can only occur through diffusion in curved geometry. To obtain this 'alpha effect' we must expand the Laplacian above as

$$\begin{aligned} \nabla^2 \mathbf{b} = {} & \mathbf{e}_\psi \nabla^2 b_\psi + \mathbf{e}_\vartheta \nabla^2 b_\vartheta + \hat{\mathbf{z}} \nabla^2 b_z \\ & + 2\nabla b_\psi \cdot \nabla \mathbf{e}_\psi + 2\nabla b_\vartheta \cdot \nabla \mathbf{e}_\vartheta + b_\psi \nabla^2 \mathbf{e}_\psi + b_\vartheta \nabla^2 \mathbf{e}_\vartheta. \end{aligned} \tag{2.12}$$

The terms appearing in the b_ψ equation are

$$\begin{aligned} \nabla\psi \cdot \nabla^2 \mathbf{b} = {} & \nabla^2 b_\psi + 2\nabla\psi \cdot (\nabla b_\psi \cdot \nabla \mathbf{e}_\psi) + 2\nabla\psi \cdot (\nabla b_\vartheta \cdot \nabla \mathbf{e}_\vartheta) \\ & + b_\psi \nabla\psi \cdot \nabla^2 \mathbf{e}_\psi + b_\vartheta \nabla\psi \cdot \nabla^2 \mathbf{e}_\vartheta. \end{aligned} \tag{2.13}$$

In the Ponomarenko dynamo the b_ψ field is small compared with the other field components at high R, as will be made explicit when we rescale variables in the next section. As a result the second and fourth terms above are certainly subdominant, leaving behind

$$\nabla\psi \cdot \nabla^2 \mathbf{b} \simeq \nabla^2 b_\psi + 2\nabla\psi \cdot (\nabla b_\vartheta \cdot \nabla \mathbf{e}_\vartheta) + b_\vartheta \nabla\psi \cdot \nabla^2 \mathbf{e}_\vartheta. \tag{2.14}$$

We need to know more of the latter two terms, and so we expand these as

$$\begin{aligned} & 2\nabla\psi \cdot (\nabla b_\vartheta \cdot \nabla \mathbf{e}_\vartheta) + b_\vartheta \nabla\psi \cdot \nabla^2 \mathbf{e}_\vartheta \\ & \qquad = \quad 2\nabla\psi \cdot (\nabla\psi \cdot \nabla \mathbf{e}_\vartheta) \partial_\psi b_\vartheta + 2\nabla\psi \cdot (\nabla\vartheta \cdot \nabla \mathbf{e}_\vartheta) \partial_\vartheta b_\vartheta \\ & \qquad\quad + 2\nabla\psi \cdot (\hat{\mathbf{z}} \cdot \nabla \mathbf{e}_\vartheta) \partial_z b_\vartheta + (\nabla\psi \cdot \nabla^2 \mathbf{e}_\vartheta) b_\vartheta \\ & \qquad \equiv \quad (2\lambda_{\mathrm{a}} \partial_\psi + 2\lambda_{\mathrm{b}} \partial_\vartheta + 2\lambda_{\mathrm{c}} \partial_z + \lambda_{\mathrm{d}}) b_\vartheta, \end{aligned} \tag{2.15}$$

using $\nabla = \nabla\psi\, \partial_\psi + \nabla\vartheta\, \partial_\vartheta + \hat{\mathbf{z}}\, \partial_z$. Here we have introduced quantities with Roman subscripts, λ_{a}–λ_{d}, which represent ways in which one might be able to regenerate b_ψ field from b_ϑ field and so close the dynamo loop.

In fact when we study the dynamo problem in the next section we will find that a solvability condition requires us to average over the angle coordinate ϑ (on a given stream line $\psi = \psi_0$). We denote this average applied to a quantity $(*)$ by $\overline{*}$ or $<*>$. Only terms possessing a non-zero average will contribute to the regeneration of field and appear in

the final equation giving the growth rate and frequency of the dynamo. We thus need to consider the quantities $\lambda_{\rm a}$, $\lambda_{\rm b}$, $\lambda_{\rm c}$ and $\lambda_{\rm d}$ and their averages over ϑ. We will find that

$$\lambda_{\rm c} = 0, \quad \overline{\lambda}_{\rm a} = \overline{\lambda}_{\rm d} = 0, \quad \overline{\lambda}_{\rm b} \equiv \alpha_m \tag{2.16}$$

and so there is only one term that has a non-vanishing average and can regenerate b_ψ field; this gives the key alpha effect term

$$\alpha_m \equiv \overline{\lambda}_{\rm b} = <\nabla\psi \cdot (\nabla\vartheta \cdot \nabla \mathbf{e}_\vartheta)>. \tag{2.17}$$

In the remainder of this subsection we prove the results in (2.16). The reader may choose instead to move directly on to the next subsection.

The result $\lambda_{\rm c} = 0$ follows immediately as $\mathbf{e}_\vartheta$ is independent of z. For averaging of $\lambda_{\rm a}$ and $\lambda_{\rm d}$ we first prove some general results about averages. Note that from (2.4), (2.10b)

$$\mathbf{e}_\vartheta \, d\vartheta = \mathbf{u}_H \, \frac{d\vartheta}{\Omega(\psi)} \, = \mathbf{u}_H \, dt = \mathbf{u}_H \, \frac{ds}{q} \, = d\mathbf{r}, \tag{2.18}$$

and

$$\nabla\psi \, d\vartheta = \Omega(\psi) \, \nabla\psi \, \frac{ds}{q} = \Omega(\psi) \, \hat{\mathbf{n}} \, ds \qquad \Big(\hat{\mathbf{n}} \equiv \frac{\nabla\psi}{|\nabla\psi|}\Big). \tag{2.19}$$

using $q \equiv |\mathbf{u}_H| = |\nabla\psi|$. This gives two useful results,

$$2\pi <\mathbf{e}_\vartheta \cdot (*)> = \oint_{\partial S_\psi} (*) \cdot d\mathbf{r} = \int_{S_\psi} \hat{\mathbf{z}} \cdot \nabla \times (*) \, dS, \tag{2.20}$$

$$2\pi <\nabla\psi \cdot (*)> = \Omega(\psi) \oint_{\partial S_\psi} (*) \cdot \hat{\mathbf{n}} \, ds = \Omega(\psi) \int_{S_\psi} \nabla \cdot (*) \, dS \tag{2.21}$$

(using Stokes' and Gauss' theorems). Here ∂S_ψ denotes the stream line, $\psi =$ const., on a horizontal plane, say $z = 0$, and S_ψ is the region inside this curve. These results are in fact equivalent (since $\mathbf{e}_\vartheta$ and $\nabla\psi$ are related by (2.10b)).

First consider $\lambda_{\rm a}$: since $\mathbf{e}_\vartheta \cdot \nabla\psi = 0$,

$$\lambda_{\rm a} \equiv \nabla\psi \cdot (\nabla\psi \cdot \nabla \mathbf{e}_\vartheta) = -\mathbf{e}_\vartheta \cdot (\nabla\psi \cdot \nabla\nabla\psi) = -\mathbf{e}_\vartheta \cdot \nabla \tfrac{1}{2}|\nabla\psi|^2. \tag{2.22}$$

It then follows from (2.20) that $\overline{\lambda}_{\rm a} = 0$. For $\lambda_{\rm d}$, recall that $\mathbf{e}_\vartheta = \Omega(\psi)^{-1}\mathbf{u}_H$ so that

$$\lambda_{\rm d} \equiv \nabla\psi \cdot \nabla^2 \mathbf{e}_\vartheta = \nabla\psi \cdot \nabla^2 \, \frac{\mathbf{u}_H}{\Omega} \, = \, \frac{1}{\Omega} \, \nabla\psi \cdot \nabla^2 \mathbf{u}_H - \frac{2\Omega'}{\Omega^2} \nabla\psi \cdot (\nabla\psi \cdot \nabla \mathbf{u}_H). \tag{2.23}$$

Using (2.21) the first of these terms averages to zero as $\nabla \cdot \mathbf{u}_H = 0$. For the second term

$$\begin{aligned} \nabla\psi \cdot (\nabla\psi \cdot \nabla \mathbf{u}_H) &= \nabla\psi \cdot (\nabla\psi \cdot \nabla(\hat{\mathbf{z}} \times \nabla\psi)) \\ &= \nabla\psi \cdot (\hat{\mathbf{z}} \times \nabla \tfrac{1}{2}|\nabla\psi|^2) = -\nabla\psi \cdot \nabla \times (\tfrac{1}{2}|\nabla\psi|^2 \hat{\mathbf{z}}). \end{aligned} \tag{2.24}$$

This averages to zero on applying (2.21).

2.3. Asymptotic analysis

We will now rescale variables in the limit $\varepsilon \to 0$ of large magnetic Reynolds number, $R = 1/\varepsilon$. In this limit the magnetic field eigenmodes become localised on stream surfaces. The stream surface for a given mode satisfies a resonance condition, that the shear in the flow on that stream surface be along the lines of constant magnetic field, at least at leading order. At this point we have a choice of how we scale the magnetic field. In the cylindrical Ponomarenko dynamo the magnetic field may be separated into modes of the form $\mathbf{b} \propto e^{im\theta+ikz+i\omega t+pt}$ in cylindrical polar coordinates (r, θ, z). Here the real frequency is ω, and the real growth rate p. Ruzmaikin *et al.* (1988) consider the scalings

$$m, k = O(1), \quad p = O(\varepsilon^{1/2}), \quad \psi = \psi_0 + O(\varepsilon^{1/4}), \tag{2.25}$$

the last equation giving the region about the resonance stream surface where the field is localised. This scaling is appropriate if one is interested in estimating the critical value of R, which will occur for modest values of m and k. However it does not capture the fastest growing modes at large R, which have the scalings

$$m, k = O(\varepsilon^{-1/3}), \quad p = O(\varepsilon^{1/3}), \quad \psi = \psi_0 + O(\varepsilon^{1/3}) \tag{2.26}$$

(Gilbert 1988).

In our analysis of generalised Ponomarenko dynamos we need to scale quantities analogously to one of these scalings. Neither is ideal, as neither scaling contains the other completely in intermediate stages of analysis, although the final results for the scaling (2.26) do include those for (2.25). We choose to use a scaling analogous to (2.25) as it is less elaborate, fewer rescaled quantities being required. The scales in ϑ and z will remain of order unity, but the growing field will be localised in a neighbourhood of width $O(\varepsilon^{1/4})$ about a stream surface $\psi = \psi_0 = \text{const.}$,

$$\psi = \psi_0 + \varepsilon^{1/4}\Psi \qquad (\Psi = O(1)). \tag{2.27}$$

We shall however retain certain subdominant terms in the Laplacian which means that our results will also be valid for the scaling analogous to (2.26) above. We are of course at liberty to do this, and we shall obtain results that are uniformly valid for all wavenumbers.

With the rescaling (2.27)

$$\nabla = \varepsilon^{-1/4}\nabla\psi\,\partial_\Psi + \nabla\vartheta\,\partial_\vartheta + \hat{\mathbf{z}}\,\partial_z. \tag{2.28}$$

We also rescale the magnetic field as in the cylindrical Ponomarenko dynamo,

$$(b_\psi, b_\vartheta, b_z)(x, y, z, t) = (\varepsilon^{1/2}B_\psi, B_\vartheta, B_z)(\Psi, \vartheta)\, e^{ikz+i\omega t+pt}. \tag{2.29}$$

The vertical wavenumber k is a parameter we are free to choose, and we will take it to be of order unity, in keeping with the scaling (2.25). The frequency and growth rate will

be functions of k and of integers m and n, introduced below, that label the modes. We expand ω and p in powers of ε as

$$\omega = \Pi_0 + \varepsilon^{1/4}\Pi_1 + \cdots, \quad p = \varepsilon^{1/2}P_0 + \cdots, \tag{2.30}$$

and expand $\Omega(\psi)$ and $W(\psi)$ about ψ_0 using (2.27) to write the scalar advection operator (2.6) as a series

$$d_t = D_0 + \varepsilon^{1/4}D_1 + \varepsilon^{1/2}D_2 + \cdots, \tag{2.31a}$$

where (assuming the field has an e^{ikz} dependence)

$$D_0 = i\Pi_0 + (\Omega_0\partial_\vartheta + ikW_0), \tag{2.31b}$$
$$D_1 = i\Pi_1 + \Psi(\Omega_0'\partial_\vartheta + ikW_0'), \tag{2.31c}$$
$$D_2 = i\Pi_2 + P_0 + \tfrac{1}{2}\Psi^2(\Omega_0''\partial_\vartheta + ikW_0''), \tag{2.31d}$$

with $\Omega_0 \equiv \Omega(\psi_0)$, $\Omega_0' \equiv \Omega'(\psi_0)$, etc.

We are left with the induction equation (2.11) in the form

$$(\varepsilon^{-1/2}d_t - \Delta_k)B_\psi = (\varepsilon^{-1/4}2\lambda_{\rm a}\partial_\Psi + 2\lambda_{\rm b}\partial_\vartheta + \lambda_{\rm d})B_\vartheta + O(\varepsilon^{1/4}), \tag{2.32a}$$
$$(\varepsilon^{-1/2}d_t - \Delta_k)B_\vartheta = \Omega_0'B_\psi + O(\varepsilon^{1/4}), \tag{2.32b}$$
$$(\varepsilon^{-1/2}d_t - \Delta_k)B_z = W_0'B_\psi + O(\varepsilon^{1/4}), \tag{2.32c}$$

using (2.12)–(2.16) and (2.28)–(2.31), with

$$\Delta_k = |\nabla\psi|^2\partial_\Psi^2 + \varepsilon^{1/4}2(\nabla\vartheta\cdot\nabla\psi)\partial_\Psi\partial_\vartheta + \varepsilon^{1/2}|\nabla\vartheta|^2\partial_\vartheta^2 - \varepsilon^{1/2}k^2. \tag{2.33}$$

As mentioned above, we have retained terms in the Laplacian (2.33) that are subdominant with the present scalings, of order $\varepsilon^{1/4}$ or $\varepsilon^{1/2}$. These terms in Δ_k all become comparable in the other scaling (2.26) and all other terms we neglect in the analysis remain subdominant. Note that also strictly we should expand $\lambda_{\rm a}$, $\lambda_{\rm b}$ and $\lambda_{\rm d}$ in a Taylor series as functions of Ψ about $\psi = \psi_0$. However it is easier not to at this point; again this can be thought of as retaining subdominant terms, and is legitimate.

Now we expand

$$B_\psi = B_{\psi0}+\varepsilon^{1/4}B_{\psi1}+\cdots, \quad B_\vartheta = B_{\vartheta0}+\varepsilon^{1/4}B_{\vartheta1}+\cdots, \quad B_z = B_{z0}+\varepsilon^{1/4}B_{z1}+\cdots, \tag{2.34}$$

and substitute this and (2.31) into (2.32). At order $\varepsilon^{-1/2}$ we have

$$D_0B_{\psi0} = D_0B_{\vartheta0} = D_0B_{z0} = 0, \tag{2.35}$$

which we solve by setting

$$(B_{\psi0}, B_{\vartheta0}, B_{z0}) = (F_\psi(\Psi), F_\vartheta(\Psi), F_z(\Psi))e^{im\vartheta} \tag{2.36}$$

and

$$i\Pi_0 + im\Omega_0 + ikW_0 = 0. \tag{2.37}$$

Here m is an integer wavenumber of order unity, which we are free to select and which labels different magnetic field modes. The frequency ω is then fixed at leading order. Rapid decay in space of the unknown functions in (2.36) as $\Psi \to \pm\infty$ is assumed. Note that once Π_0 is fixed by (2.37), the operator D_0 annihilates the function $e^{im\vartheta}$.

At the next order we have

$$D_0 B_{\psi 1} + D_1 B_{\psi 0} = 2\lambda_{\rm a}\partial_\Psi B_{\vartheta 0}, \quad D_0 B_{\vartheta 1} + D_1 B_{\vartheta 0} = 0, \quad D_0 B_{z1} + D_1 B_{z0} = 0. \quad (2.38\text{a,b,c})$$

To solve these, we shall first set

$$im\Omega_0' + ikW_0' = 0, \quad \Pi_1 = 0. \quad (2.39)$$

The first of these removes the term linear in Ψ in D_1 and d_t; this means that we are minimising the destructive effect of differential advection. It is also a 'resonance' condition fixing the stream surface $\psi = \psi_0$ in terms of m and k. In short, having fixed m and k this condition tells us where that mode will localise (assuming there is such a surface in the flow). Once (2.39) is applied D_1 annihilates terms in $e^{im\vartheta}$ and the terms involving D_1 in (2.38) are zero by (2.36).

Equations (2.38b,c) may now be solved in a similar form to (2.36), and this leaves equation (2.38a) for $B_{\psi 1}$ which has a source term

$$D_0 B_{\psi 1} = 2\lambda_{\rm a}\partial_\Psi B_{\vartheta 0} = 2\lambda_{\rm a} F_\vartheta'(\Psi) e^{im\vartheta}. \quad (2.40)$$

This equation has a solvability condition; from (2.31b) and (2.37) it is required that there be no component in $e^{im\vartheta}$ on the right-hand side, which is the case since $\overline{\lambda}_{\rm a} = 0$ from (2.16). As a result the equation for $B_{\psi 1}$ can be solved and the particular integral may be written in the form $H(\Psi,\vartheta)e^{im\vartheta}$. We may write the solution to the full first order system as

$$(B_{\psi 1}, B_{\vartheta 1}, B_{z1}) = (G_\psi(\Psi) + H(\Psi,\vartheta), G_\vartheta(\Psi), G_z(\Psi))e^{im\vartheta}, \quad <H(\Psi,\vartheta)> = 0. \quad (2.41)$$

We now move to the important terms of order one in equations (2.32), which are:

$$D_0 B_{\psi 2} + D_1 B_{\psi 1} + (D_2 - \Delta_k) B_{\psi 0} = 2\lambda_{\rm a}\partial_\Psi B_{\vartheta 1} + 2\lambda_{\rm b}\partial_\vartheta B_{\vartheta 0} + \lambda_{\rm d} B_{\vartheta 0}, \quad (2.42\text{a})$$

$$D_0 B_{\vartheta 2} + D_1 B_{\vartheta 1} + (D_2 - \Delta_k) B_{\vartheta 0} = \Omega_0' B_{\psi 0}, \quad (2.42\text{b})$$

$$D_0 B_{z2} + D_1 B_{z1} + (D_2 - \Delta_k) B_{z0} = W_0' B_{\psi 0}. \quad (2.42\text{c})$$

Again solvability of these equations for the B_2 fields requires that the sums of the remaining terms have no $e^{im\vartheta}$ harmonic; this is guaranteed for the terms $D_1 B_{\psi 1}$, $D_1 B_{\vartheta 1}$ and $D_1 B_{z1}$. Also the terms $\lambda_{\rm a}\partial_\Psi B_{\vartheta 1}$ and $\lambda_{\rm d} B_{\vartheta 0}$ have no term in $e^{im\vartheta}$, from (2.16), (2.36) and (2.41). Thus using (2.31d), (2.33) and (2.36), solvability requires that

$$\Xi F_\psi = 2im\alpha_m F_\vartheta, \quad \Xi F_\vartheta = \Omega_0' F_\psi, \quad \Xi F_z = W_0' F_\psi \quad (2.43\text{a,b,c})$$

(we recall that $\overline{\lambda}_{\rm b} = \alpha_m$), with

$$\Xi \equiv i\Pi_2 + P_0 + \tfrac{1}{2}\Psi^2(im\Omega_0'' + ikW_0'') - \Delta_{mk}, \quad (2.44)$$

$$\Delta_{mk} = <|\nabla\psi|^2>\partial_\Psi^2 + \varepsilon^{1/4}2im<\nabla\vartheta\cdot\nabla\psi>\partial_\Psi - \varepsilon^{1/2}m^2<|\nabla\vartheta|^2> - \varepsilon^{1/2}k^2. \tag{2.45}$$

α_m may be identified with an alpha effect and may be evaluated by the line integral (2.17) taken along the curve $\psi = \psi_0$ at this order.

The equations (2.43) above are coupled parabolic cylinder equations. We may combine the first two of these as

$$(\Xi^2 - 2im\alpha_m\Omega_0')F_\psi = (\Xi + \sqrt{2im\alpha_m\Omega_0'})(\Xi - \sqrt{2im\alpha_m\Omega_0'})F_\psi = 0. \tag{2.46}$$

The canonical form for a parabolic cylinder equation is $y''(x) - (\frac{1}{4}x^2 + a)y(x) = 0$ and this has solutions decaying as $x \to \pm\infty$ provided $a = -n - \frac{1}{2}$ with $n = 0, 1, 2, \ldots$ (see Abramowitz & Stegun 1965, chapter 19). This together with (2.44) and (2.45) above fixes the growth rates, after some straightforward calculations,

$$i\Pi_2 + P_0 + \varepsilon^{1/2}(\beta_m m^2 + k^2) \mp \sqrt{2im\alpha_m\Omega_0'} = -(n+\tfrac{1}{2})\sqrt{2i\gamma(m\Omega_0'' + kW_0'')} \tag{2.47}$$

with

$$\beta_m = <|\nabla\vartheta|^2> - \gamma^{-1}<\nabla\vartheta\cdot\nabla\psi>^2, \quad \gamma = <|\nabla\psi|^2>. \tag{2.48}$$

The corresponding eigenfunction for $n = 0$ takes the form

$$F_\psi, F_\vartheta, F_z \propto \exp\Big(-\tfrac{1}{4}\Psi^2\sqrt{2i\gamma^{-1}(m\Omega_0'' + kW_0'')} - \varepsilon^{1/4}im\gamma^{-1}<\nabla\vartheta\cdot\nabla\psi>\Psi\Big). \tag{2.49}$$

2.4. Summary

Taking the real and imaginary parts of (2.47) and returning to unscaled quantities (see (2.30)), we obtain the Ponomarenko dynamo growth rate given by

$$p \sim \pm\sqrt{\varepsilon|m\alpha_m\Omega_0'|} - (n+\tfrac{1}{2})\sqrt{\varepsilon\gamma|m\Omega_0'' + kW_0''|} - \varepsilon(\beta_m m^2 + k^2). \tag{2.50}$$

The frequency is

$$\begin{aligned}\omega \sim {} & -im\Omega_0 - ikW_0 \\ & \pm\sqrt{\varepsilon|m\alpha_m\Omega_0'|}\,\mathrm{sign}(m\alpha_m\Omega_0') - (n+\tfrac{1}{2})\sqrt{\varepsilon\gamma|m\Omega_0'' + kW_0''|}\,\mathrm{sign}(m\Omega_0'' + kW_0''),\end{aligned} \tag{2.51}$$

with

$$\alpha_m = <\nabla\psi\cdot(\nabla\vartheta\cdot\nabla\mathbf{e}_\vartheta)>, \tag{2.52a}$$

$$\beta_m = <|\nabla\vartheta|^2> - \gamma^{-1}<\nabla\vartheta\cdot\nabla\psi>^2, \qquad \gamma = <|\nabla\psi|^2>. \tag{2.52b,c}$$

These expressions are uniformly valid for all m, k and include the two scalings (2.25) and (2.26). The averages are taken over the stream surface $\psi = \psi_0$ on which the resonance condition (2.39) holds (assuming such a surface exists).

The analysis is valid provided the eigenfunction is localised as assumed, in other words provided that on the stream surface

$$m\Omega_0'' + kW_0'' \neq 0. \tag{2.53}$$

If this assumption is not satisfied, it is plausible that dynamo action will still occur (as the Ponomarenko mechanism is still present), but the field will be less localised, and further analysis is necessary (see Ruzmaikin *et al.* 1988). Note that for dynamo action to occur it is necessary that $m \neq 0$ and $\Omega_0' \neq 0$ from (2.50), and from (2.39) it then follows that $k \neq 0$ and $W_0' \neq 0$.

The result for the growth rate generalises that given by Gilbert (1988) and Ruzmaikin *et al.* (1988) and takes a very similar form. The first term in (2.50) is the dynamo generation term, including the stretching by differential rotation and the alpha effect. The second term can be thought of as an eddy diffusion term: the changing pitch of the stream lines near the surface $\psi = \psi_0$ tends to enhance diffusion of field, and leads to this negative-definite term. The third term is simply molecular diffusion, averaged over the stream surface.

At large R we also obtain a criterion for dynamo action. The first and second terms in (2.50) scale in the same way with m and ϵ and so are always comparable. However the third term can be made negligible, for example by fixing m as $\varepsilon \to 0$. Thus a necessary and sufficient condition (within this asymptotic framework) for dynamo action at high R is that the sum of the first two terms be positive. This gives a geometrical criterion, that on a given stream surface

$$\frac{\gamma}{4}\left|\frac{\Omega''(\psi)}{\Omega'(\psi)} - \frac{W''(\psi)}{W'(\psi)}\right| \equiv \frac{\gamma}{4}\left|\frac{d}{d\psi}\log\left|\frac{\Omega'(\psi)}{W'(\psi)}\right|\right| < |\alpha_m| \tag{2.54}$$

for dynamo action to occur at high R. This again generalises immediately the dynamo criterion of Gilbert (1988) and Ruzmakin *et al.* (1988). The localisation condition (2.53) amounts to the condition that the quantity on the left-hand side of the inequality (2.54) should not vanish.

3. Cartesian geometry with general vertical velocity $W(x, y)$

In this section we generalise the results of section 2 by allowing the vertical velocity W to have an arbitrary, but smooth dependence in the plane, $W = W(x, y)$, rather than being restricted to be constant on stream surfaces. Looking back through section 2, the effect of allowing a general W is that the advection operator in the form (2.6) gains a dependence on ϑ as well as ψ. This is undesirable, and our approach is to introduce a coordinate change so that d_t again only depends on ψ. Once this is done, all the complications of the coordinate system are again pushed into the Laplacian. In this section we will not go into as much detail as before; we will sketch our calculations and only highlight important differences from section 2.

3.1. Geometry and asymptotics

We define an angle coordinate ϑ as before, and can then write the vertical velocity as $W = W(\psi, \vartheta)$. We split this up into mean and fluctuating components

$$W(x, y) = W(\psi, \vartheta) = \overline{W}(\psi) + \widetilde{W}(\psi, \vartheta), \tag{3.1}$$

where, as always, the bar denotes an average over ϑ. We now remove the ϑ-dependence in d_t by changing coordinates from (ψ, ϑ, z) to (ψ, ϑ, ζ) with $\zeta = \zeta(\psi, \vartheta, z)$. Under a transformation of this type

$$d_t \equiv \partial_t + \Omega(\psi)\partial_\vartheta + W(\psi,\vartheta)\partial_z = \partial_t + \Omega(\psi)\partial_\vartheta + \Big(\Omega(\psi)\,\frac{\partial\zeta}{\partial\vartheta} + W(\psi,\vartheta)\frac{\partial\zeta}{\partial z}\Big)\partial_\zeta. \tag{3.2}$$

Let us define the new coordinate ζ by

$$\zeta(\psi,\vartheta,z) = z - Z(\psi,\vartheta), \qquad Z(\psi,\vartheta) = \Omega(\psi)^{-1}\int_0^\vartheta \widetilde{W}(\psi,\sigma)\,d\sigma. \tag{3.3}$$

Using ζ in place of z corresponds to replacing horizontal surfaces of constant z by distorted horizontal surfaces $\zeta = \text{const}$. Note that no secular effects are introduced as it may be verified that $|\nabla\zeta|$ is always bounded. With respect to these distorted surfaces a fluid element moves uniformly with a vertical velocity $\overline{W}(\psi)$. We have

$$\dot\psi = 0, \quad \dot\vartheta = \Omega(\psi), \quad \dot\zeta = \overline{W}(\psi) \tag{3.4}$$

and the advection operator is

$$d_t = \partial_t + \Omega(\psi)\partial_\vartheta + \overline{W}(\psi)\partial_\zeta \tag{3.5}$$

as required.

We now use the basis $\{\nabla\psi, \nabla\vartheta, \nabla\zeta\}$ to measure field components b_ψ, b_ϑ and b_ζ (cf. (2.7)). In this new basis $\nabla\psi$ and $\nabla\vartheta$ are unchanged from the basis used in section 2. However the third basis vector,

$$\nabla\zeta = \hat{\mathbf{z}} - \nabla Z = \hat{\mathbf{z}} - \partial_\psi Z\,\nabla\psi - \partial_\vartheta Z\,\nabla\vartheta, \tag{3.6}$$

now has horizontal components. Equation (2.9) here yields

$$\nabla\psi\times\nabla\vartheta\cdot\nabla\zeta = \nabla\psi\times\nabla\vartheta\cdot\hat{\mathbf{z}} = \Omega(\psi), \tag{3.7}$$

and so the reciprocal basis is $\{\mathbf{f}_\psi, \mathbf{f}_\vartheta, \hat{\mathbf{z}}\}$ with

$$\mathbf{f}_\psi = \mathbf{e}_\psi + \hat{\mathbf{z}}\,\partial_\psi Z, \qquad \mathbf{f}_\vartheta = \mathbf{e}_\vartheta + \hat{\mathbf{z}}\,\partial_\vartheta Z = \Omega(\psi)^{-1}(\mathbf{u}_H + \widetilde{W}\,\hat{\mathbf{z}}). \tag{3.8}$$

Writing $\mathbf{b} = b_\psi\mathbf{f}_\psi + b_\vartheta\mathbf{f}_\vartheta + b_\zeta\hat{\mathbf{z}}$, from (3.4) these magnetic field components obey

$$d_t b_\psi = \varepsilon\nabla\psi\cdot\nabla^2\mathbf{b}, \tag{3.9a}$$

$$d_t b_\vartheta - \Omega'(\psi)b_\psi = \varepsilon\nabla\vartheta\cdot\nabla^2\mathbf{b}, \tag{3.9b}$$

$$d_t b_\zeta - \overline{W}'(\psi)b_\psi = \varepsilon\nabla\zeta\cdot\nabla^2\mathbf{b}. \tag{3.9c}$$

Again the important issue is to track down terms with non-zero mean that generate b_ψ field from b_ϑ field. (Helpfully, there are no source terms from the b_ζ field.) The relevant terms are

$$\begin{aligned}
&\nabla\psi\cdot(2\nabla b_\vartheta\cdot\nabla\mathbf{f}_\vartheta + b_\vartheta\nabla^2\mathbf{f}_\vartheta)\\
&\quad= \quad 2\nabla\psi\cdot(\nabla\psi\cdot\nabla\mathbf{f}_\vartheta)\partial_\psi b_\vartheta + 2\nabla\psi\cdot(\nabla\vartheta\cdot\nabla\mathbf{f}_\vartheta)\partial_\vartheta b_\vartheta && \text{(3.10a,b)}\\
&\qquad + 2\nabla\psi\cdot(\nabla\zeta\cdot\nabla\mathbf{f}_\vartheta)\partial_\zeta b_\vartheta \quad + (\nabla\psi\cdot\nabla^2\mathbf{f}_\vartheta)b_\vartheta && \text{(3.10c,d)}\\
&\quad\equiv \quad (2\mu_{\rm a}\partial_\psi + 2\mu_{\rm b}\partial_\vartheta + 2\mu_{\rm c}\partial_\zeta + \mu_{\rm d})b_\vartheta,
\end{aligned}$$

where we introduce coefficients $\mu_{\rm a}$–$\mu_{\rm d}$ analogous to $\lambda_{\rm a}$–$\lambda_{\rm d}$ in (2.15). Their properties may be summarized by

$$\overline{\mu}_{\rm a} = \overline{\mu}_{\rm d} = 0, \quad \overline{\mu}_{\rm b} \equiv \alpha_m, \quad \overline{\mu}_{\rm c} \equiv \alpha_k. \tag{3.11}$$

There are two non-zero alpha effect terms; the first is

$$\alpha_m \equiv \overline{\mu}_{\rm b} = <\nabla\psi\cdot(\nabla\vartheta\cdot\nabla\mathbf{f}_\vartheta)> \tag{3.12}$$

which from (3.8) simplifies to

$$\alpha_m = <\nabla\psi\cdot(\nabla\vartheta\cdot\nabla\mathbf{e}_\vartheta)> = \overline{\lambda}_{\rm b}. \tag{3.13}$$

This is the same alpha effect as identified in section 2 in equation (2.17), and is independent of the form of the vertical velocity W. The second term is new:

$$\alpha_k \equiv \overline{\mu}_{\rm c} = <\nabla\psi\cdot(\nabla\zeta\cdot\nabla\mathbf{f}_\vartheta)>. \tag{3.14}$$

Using (3.6) and (3.8), this may be rewritten as

$$\begin{aligned}
\alpha_k &= <\nabla\psi\cdot(\nabla\zeta\cdot\nabla\mathbf{e}_\vartheta)>\\
&= -<\nabla\psi\cdot(\nabla\psi\cdot\nabla\mathbf{e}_\vartheta)\partial_\psi Z> - <\nabla\psi\cdot(\nabla\vartheta\cdot\nabla\mathbf{e}_\vartheta)\partial_\vartheta Z> \qquad (3.15)\\
&= -<\lambda_{\rm a}\partial_\psi Z> - <\lambda_{\rm b}\partial_\vartheta Z>.
\end{aligned}$$

Here the distorted surfaces of constant ζ lead to terms which contribute to the new alpha effect, coupling ϑ-field to ψ-field. The first term involves a weighted average of $\lambda_{\rm a}$, and although $\overline{\lambda}_{\rm a} = 0$, this average need not be zero. The point here is that the non-uniform vertical velocity can tilt magnetic field transverse to stream surfaces and give a net effect. The second term involves $\lambda_{\rm b}$; here $\overline{\lambda}_{\rm b} = \alpha_m \neq 0$ in general in any case, but the effect of non-uniform vertical motion is to tilt field along stream surfaces and give an extra contribution.

For the remaining terms,

$$\mu_{\rm a} \equiv \nabla\psi\cdot(\nabla\psi\cdot\nabla\mathbf{f}_\vartheta) = \nabla\psi\cdot(\nabla\psi\cdot\nabla\mathbf{e}_\vartheta) = \lambda_{\rm a}, \tag{3.16}$$

which averages to zero. Finally we have

$$\mu_{\rm d} = \nabla\psi\cdot\nabla^2\mathbf{f}_\vartheta = \nabla\psi\cdot\nabla^2\mathbf{e}_\vartheta + \nabla\psi\cdot\nabla^2(\partial_\vartheta Z\,\hat{\mathbf{z}}) = \nabla\psi\cdot\nabla^2\mathbf{e}_\vartheta = \lambda_{\rm d} \tag{3.17}$$

and this averages to zero as before.

The remaining theory goes through similarly to section 2.3 with minor modifications, in particular the replacement of z by ζ and W by $\overline{W}$. The Laplacians in equations (2.33) and (2.45) acquire extra cross terms, which we do not list here for brevity. Equation (2.32a) has an extra term $2ik\mu_c B_\vartheta$ on the right-hand side, and similarly for equation (2.42a). The coupled parabolic cylinder equations (2.43) become

$$\Xi F_\psi = 2i(m\alpha_m + k\alpha_k)F_\vartheta, \qquad \Xi F_\vartheta = \Omega_0' F_\psi, \qquad \Xi F_\zeta = \overline{W}_0' F_\psi, \tag{3.18a,b,c}$$

and are solved *mutatis mutandis* as those in section 2.

3.2. Summary

We finally obtain the growth rate for the case of general vertical velocity $W(x,y)$ as

$$p \sim \pm\sqrt{\varepsilon|m\alpha_m + k\alpha_k||\Omega_0'|} - (n+\tfrac{1}{2})\sqrt{\varepsilon\gamma|m\Omega_0'' + k\overline{W}_0''|} - \varepsilon(\beta_m m^2 + \beta_k k^2 + 2\beta_{mk}mk), \tag{3.19}$$

with

$$\alpha_m = <\nabla\psi\cdot(\nabla\vartheta\cdot\nabla\mathbf{e}_\vartheta)>, \qquad \alpha_k = <\nabla\psi\cdot(\nabla\zeta\cdot\nabla\mathbf{e}_\vartheta)>, \tag{3.20a,b}$$

$$\beta_m = <|\nabla\vartheta|^2> - \gamma^{-1}<\nabla\vartheta\cdot\nabla\psi>^2, \tag{3.20c}$$

$$\beta_k = <|\nabla\zeta|^2> - \gamma^{-1}<\nabla\zeta\cdot\nabla\psi>^2, \tag{3.20d}$$

$$\beta_{mk} = <\nabla\vartheta\cdot\nabla\zeta> - \gamma^{-1}<\nabla\vartheta\cdot\nabla\psi><\nabla\zeta\cdot\nabla\psi>, \tag{3.20e}$$

$$\gamma = <|\nabla\psi|^2>, \tag{3.20f}$$

all averaged over the stream line $\psi = \psi_0$. It is also required that

$$m\Omega_0' + k\overline{W}_0' = 0, \qquad m\Omega_0'' + k\overline{W}_0'' \neq 0, \tag{3.21a,b}$$

on the stream surface. In the growth rate (3.19) the first term gives the two alpha effects, the constant α_m being the same as in section 2, while the constant α_k arises from the non-uniform vertical velocity.

For growing modes it is required that $k \neq 0$ (for if $k = 0$ then from (3.21a) m or Ω_0' is zero and the dynamo fails by (3.19) as the first term is zero). There are then two possibilities: first, if $\overline{W}_0' \neq 0$ on the resonant surface, then necessarily $m \neq 0$ and $\Omega_0' \neq 0$ and the criterion for dynamo action on the surface becomes

$$\frac{\gamma}{4}\left|\frac{\Omega''(\psi)}{\Omega'(\psi)} - \frac{\overline{W}''(\psi}{\overline{W}'(\psi)}\right| \equiv \frac{\gamma}{4}\left|\frac{d}{d\psi}\log\left|\frac{\Omega'(\psi)}{\overline{W}'(\psi)}\right|\right| < \left|\alpha_m - \frac{\Omega'(\psi)}{\overline{W}'(\psi)}\,\alpha_k\right|, \tag{3.22}$$

similar to the earlier result (2.54). However another possibility is that $\overline{W}_0' = 0$ on the resonant surface and then dynamo action can occur with $m = 0$, $k \neq 0$ and $\Omega_0' \neq 0$ (and we also require $\overline{W}_0'' \neq 0$ for localisation). In this case the dynamo criterion simplifies to

$$\frac{\gamma}{4}\left|\frac{\overline{W}''(\psi)}{\Omega'(\psi)}\right| < |\alpha_k|. \tag{3.23}$$

Note that in this case $m = 0$, the magnetic field still depends on both ϑ and z through ζ.

4. Example of elliptical stream lines

We illustrate the theory of sections 2 and 3 by giving an example where the alpha effects may be obtained analytically. In this way we confirm that the new alpha effect we obtain is generally non-zero, and can see how it arises in a simple situation. We also obtain a criterion for dynamo action at high R in this class of flows.

Consider a general smooth flow having elliptical stream lines (cf. Bassom & Gilbert 2000). Let a family of concentric ellipses in the (x, y)-plane be given by level curves of $\eta = ax^2 + by^2$. We define a flow around these ellipses by setting

$$\psi = f(\eta), \quad \mathbf{u}_H = f'(\eta)\,(-2by, 2ax, 0), \tag{4.1}$$

where f is any smooth function with $f'(\eta)$ nowhere zero. Here the bracket notation refers to components of vectors with respect to the Cartesian unit vectors $\{\hat{\mathbf{x}}, \hat{\mathbf{y}}, \hat{\mathbf{z}}\}$. The angle coordinate ϑ is defined by

$$x = \sqrt{\eta/a}\cos\vartheta, \quad y = \sqrt{\eta/b}\sin\vartheta, \tag{4.2}$$

and the angular velocity is $\Omega(\psi) = 2\sqrt{ab}\,f'(\eta)$. This defines the flow in the horizontal plane. Now we introduce the vertical velocity. It is sufficient to introduce a mean flow and a harmonic in 2ϑ (other harmonics would not contribute to the dynamo process after averaging),

$$W = \overline{W}(\psi) + \widetilde{W}(\psi, \vartheta) = g(\eta) + h(\eta)\cos 2\vartheta + j(\eta)\sin 2\vartheta. \tag{4.3}$$

The ζ coordinate is defined from (3.3),

$$\zeta = z - Z(\psi, \vartheta), \quad Z = \tfrac{1}{2}\Omega(\psi)^{-1}(h(\eta)\sin 2\vartheta - j(\eta)\cos 2\vartheta). \tag{4.4}$$

(Note that we have discarded a function of η in integrating (3.3) to obtain Z; this may be done as the lower limit in (3.3) is irrelevant). This gives the non-trivial basis vectors as

$$\nabla\psi = (2ax, 2by, 0)f'(\eta), \quad \nabla\vartheta = \eta^{-1}\sqrt{ab}\,(-y, x, 0), \tag{4.5a,b}$$

$$\nabla\zeta = \hat{\mathbf{z}} - \partial_\psi Z\,\nabla\psi - \Omega^{-1}\widetilde{W}\nabla\vartheta, \tag{4.5c}$$

$$\mathbf{f}_\psi = \mathbf{e}_\psi + \partial_\psi Z\,\hat{\mathbf{z}}, \quad \mathbf{f}_\vartheta = \mathbf{e}_\vartheta + \Omega^{-1}\widetilde{W}\hat{\mathbf{z}} = \Omega^{-1}(\mathbf{u}_H + \widetilde{W}\hat{\mathbf{z}}), \tag{4.5d,e}$$

with

$$\mathbf{e}_\psi = \Omega^{-1}\eta^{-1}\sqrt{ab}\,(x, y, 0), \qquad \mathbf{e}_\vartheta = \Omega^{-1}\mathbf{u}_H = (ab)^{-1/2}(-by, ax, 0). \tag{4.6}$$

Now from these results it may be verified that

$$\lambda_{\mathrm{a}} \equiv \nabla\psi\cdot(\nabla\psi\cdot\nabla\mathbf{e}_\vartheta) = 4\sqrt{ab}(a-b)xyf'(\eta)^2, \tag{4.7a}$$

$$\lambda_{\mathrm{b}} \equiv \nabla\psi\cdot(\nabla\vartheta\cdot\nabla\mathbf{e}_\vartheta) = -2\eta^{-1}ab(x^2+y^2)f'(\eta). \tag{4.7b}$$

Substituting for x and y from (4.2) above and averaging over ϑ gives the first alpha effect term as

$$\alpha_m = \overline{\lambda}_{\mathrm{b}} = -(a+b)f'(\eta) \tag{4.8a}$$

from (3.13). After some calculations the second alpha effect term may be written as

$$\alpha_k = -<\lambda_{\rm a}\partial_\psi Z> - <\lambda_{\rm b}\partial_\vartheta Z> = \frac{(b-a)f'(\eta)}{4\sqrt{ab}}\,\frac{d}{d\eta}\Big(\frac{\eta h(\eta)}{f'(\eta)}\Big). \tag{4.8b}$$

(from (3.15)). This is the alpha effect term from the non-uniform vertical velocity, and vanishes if $h(\eta) = 0$ or if the stream lines are circular, $a = b$.

The criterion (3.22) for high-R dynamo action becomes

$$\eta(a+b)\,\Big|\frac{f'''}{f''} - \frac{g''}{g'}\Big| < \Big|2(a+b) + (b-a)\,\frac{f''}{g'}\Big(\frac{\eta h}{f'}\Big)'\Big| \tag{4.9}$$

for $m \neq 0$. For a surface with $g'(\eta) = 0$, the criterion for $m = 0$ modes is, from (3.23),

$$\Big|\eta(a+b)\,\frac{g''}{f''}\Big| < \Big|(b-a)\Big(\frac{\eta h}{f'}\Big)'\Big|. \tag{4.10}$$

5. Numerical confirmation

5.1. Comparison of theory and simulation

We have confirmed the asymptotic theory developed so far in this paper by means of direct numerical simulation of the induction equation (2.1) for chosen flow fields. We shall consider the stream function

$$\psi = \sin x \cos(\pi y/2), \tag{5.1}$$

shown in figure 3(a), and two choices of vertical velocity W

$$W_1 = \cos^2 x + y^2, \qquad W_2 = (1-\sin^2 x)\sqrt{1-y^2}, \tag{5.2}$$

shown in figures 3(b,c). For direct numerical simulations a spectral code is used to integrate the induction equation in a plane layer with $-1 \le y \le 1$ (using insulating boundary conditions) and periodic in x with period 2π. The code is described further in Ponty *et al.* (2000).

Figure 4 shows the dynamo growth rate p as a function of $\log_{10} R$ for the flow given by ψ and W_1 with $k = 0.7$. The numerical results are markers joined by a dashed line; the asymptotic results of this paper are the solid line. Good agreement is seen, as R is increased. The mode is an $m = 1$ mode (this emerges from the simulation), and the magnetic field is shown in three dimensions in figure 5. According to our calculations (explained further below) this mode should localise on the stream surface given by $\psi \simeq 0.549$, and the corresponding alpha effects are $\alpha_m \simeq 1.35$ and $\alpha_k \simeq -0.061$. For this case the α_k effect is virtually negligible in the combination $m\alpha_m + k\alpha_k$; so while the numerical results for this flow are a good test of the analysis of section 2, to test section 3 we were led to devise our second example.

In this example the flow is given by ψ and W_2, and the mode with $m = 1$, $k = 1.5$ localises on the stream surface given by by $\psi_0 \simeq 0.529$. The corresponding alpha effects are $\alpha_m \simeq 1.34$ and $\alpha_k \simeq -0.15$. This provides a reasonable test of our analytical calculation of α_k. Numerical and analytical growth rates are plotted in figure 6. The numerical results show three magnetic modes which are dominant in different ranges of R. In the range $400 \lesssim R \lesssim 1100$ the simulations show an $m = 1$ Ponomarenko mode and there is good agreement between the theory and the simulation. The field is shown in figure 7 for $R = 500$. For $R \lesssim 300$ or $R \gtrsim 1250$ there are other modes, in which the magnetic field is associated with the stagnation points on the boundary and their connecting separatrices. Our analysis cannot capture these modes, one of which is depicted in figure 8.

As a final example we consider the flow discussed by Plunian *et al.* (1999) which models the flow of liquid sodium in a fast breeder reactor. In our notation the flow is

$$\psi = -2^{-3/2}(1 + \cos x)(1 + \cos y), \qquad W = -\psi/2 \tag{5.3}$$

and has a network of square cells in which the fluid rotates and moves vertically with the same sense in each cell. Plunian *et al.* (1999) find two dynamo mechanisms at work, the Ponomarenko mechanism, and a Roberts dynamo mechanism in which the field is localised on the cell boundaries (see Roberts 1970, Childress 1979, Soward 1987). Our aim is to reproduce the results for the Ponomarenko mechanism only, shown in their figure 9 which gives the critical value R_c for dynamo action as a function of the wavenumber k.

Our figure 9 gives a comparison between their results† (markers and dotted lines) and our results (solid lines). The different curves correspond to values of m from 1 to 5, reading from left to right. Satisfactory agreement is seen overall, in particular for the lowest critical values of R_c for each mode, and for the higher m-values. The V-shaped theoretical curves are all related, since from (3.19) it may be checked that $R_c(m, k) = m^3 R_c(1, k/m)$ for our approximation. Although the Roberts mechanism dominates for certain k values, we have not reproduced the critical curves on figure 9 for clarity, and refer the reader to figure 9 of Plunian *et al.* (1999) for this additional information.

Note that as R_c increases for the left side of each V-shaped curve, the dynamo mode becomes localised closer to the elliptical stagnation point (of $\mathbf{u}_H$) at the centre of each cell. On the right side of each V-shaped curve, the critical mode becomes localised closer to the separatrices bounding each cell. The theory assumes that the dynamo modes are isolated away from points in which $\mathbf{u}_H$ is zero, and this appears to be the reason why the agreement does not improve significantly as one increases R_c for each value of m.

We have not sought to extend the results of Plunian *et al.* (1999), as the thrust of the present paper is the asymptotic theory. We note however that our asymptotics could be useful in surveying the possibility of Ponomarenko dynamo action in wide classes of flows, supported by full numerical simulations. Although our results are only asymptotic, a robust criterion for validity could be devised, as the field is localised within a region whose width $\delta\psi$ may be deduced from (2.49). It is required that this width be small compared with the variation of ψ in the flow, and that the region where the field is localised should not overlap elliptic or hyperbolic stagnation points in $\mathbf{u}_H$.

† The data points for $m = 1$ differ in detail from those in Plunian *et al.* (1999), as they have since been recalculated to greater accuracy by Dr. F. Plunian.

5.2. Asymptotic calculations for specific examples

The asymptotic growth rates shown in figures 4, 6 and 9 are given by equation (3.19), but this involves a number of quantities in (3.20) which are given by an average over the resonant stream surface. These must be obtained numerically for any but the simplest flows, and in this section we indicate how this was done. The programs use a subroutine from the NAG library that integrates first order equations by a variable-step, variable-order Adams method.

We begin with a flow and values of the wavenumbers m and k for the dynamo mode we wish to explore. We make a guess at the location of the resonant stream surface $\psi = \psi_0$. We fix three closed stream lines with ψ equal to ψ_0, $\psi_0 \pm \delta\psi$ with $\delta\psi \ll 1$ fixed, and for each of these three we integrate the equations

$$\dot{x} = -\partial_y \psi, \quad \dot{y} = \partial_x \psi, \quad \dot{z} = W, \tag{5.4}$$

around one complete circuit in the (x, y)-plane. For each stream line the period T and the total change $[z]$ in the vertical coordinate fix $\Omega(\psi) = 2\pi/T$ and $\overline{W}(\psi) = [z]/T$ respectively. From this we may calculate Ω_0, Ω_0', Ω_0'', $\overline{W}_0$, $\overline{W}_0'$ and $\overline{W}_0''$ using finite differencing in ψ. Knowing Ω_0' and $\overline{W}_0'$ we make use of the resonance condition $m\Omega_0' + k\overline{W}_0' = 0$. This will generally not be satisfied with our initial guess for ψ_0, but we may then iterate on ψ_0 to find the stream surface satisfying the resonance condition to any given accuracy.

Once the surface $\psi = \psi_0$, m and k are all fixed, we integrate again to obtain x, y and Z as functions of ϑ rather than time:

$$dx/d\vartheta = -\Omega(\psi)^{-1}\partial_y \psi, \quad dy/d\vartheta = \Omega(\psi)^{-1}\partial_x \psi, \quad dZ/d\vartheta = \Omega(\psi)^{-1}\widetilde{W}. \tag{5.5}$$

We do this for each of the three stream lines, so that we have a good local approximation to $x(\psi, \vartheta)$, $y(\psi, \vartheta)$ and $Z(\psi, \vartheta)$.

At each point on the stream line we can obtain the Jacobian matrix $\partial(x, y)/\partial(\psi, \vartheta)$ by finite differences and compute its inverse $\partial(\psi, \vartheta)/\partial(x, y)$. This gives the vectors $\nabla\psi$, $\nabla\vartheta$, $\mathbf{e}_\psi = \partial_\psi x\, \hat{\mathbf{x}} + \partial_\psi y\, \hat{\mathbf{y}}$ and $\mathbf{e}_\vartheta = \partial_\vartheta x\, \hat{\mathbf{x}} + \partial_\vartheta y\, \hat{\mathbf{y}}$. We can also obtain $\partial_\psi Z$ and $\partial_\vartheta Z$ at each point on the stream line and so form $\mathbf{f}_\psi$, $\mathbf{f}_\vartheta$ and $\nabla\zeta$ using (3.6) and (3.8). With these calculations we know the bases $\{\nabla\psi, \nabla\vartheta, \nabla\zeta\}$ and $\{\mathbf{f}_\psi, \mathbf{f}_\vartheta, \hat{\mathbf{z}}\}$ at each point, in terms of the unit vectors $\{\hat{\mathbf{x}}, \hat{\mathbf{y}}, \hat{\mathbf{z}}\}$. As checks on this computation we recall that we know $\nabla\psi$ and $\Omega(\psi)\mathbf{f}_\vartheta = \mathbf{u}_H + \widetilde{W}\,\hat{\mathbf{z}}$ analytically and that (3.7) also provides a check.

We can now calculate the various quantities we need for the growth rate. We can measure $<|\nabla\psi|^2>$, $<|\nabla\vartheta|^2>$, $<|\nabla\zeta|^2>$, $<\nabla\psi\cdot\nabla\vartheta>$, $<\nabla\psi\cdot\nabla\zeta>$ and $<\nabla\vartheta\cdot\nabla\zeta>$ by averaging around the stream line $\psi = \psi_0$, which provides the β-terms in (3.20). To compute the alpha effect terms we write these in the form

$$\alpha_m = <\nabla\psi\cdot(\nabla\vartheta\cdot\nabla\mathbf{f}_\vartheta)> = -<\mathbf{f}_\vartheta\cdot(\nabla\vartheta\cdot\nabla\nabla\psi)>, \tag{5.6a}$$

$$\alpha_k = <\nabla\psi\cdot(\nabla\zeta\cdot\nabla\mathbf{f}_\vartheta)> = -<\mathbf{f}_\vartheta\cdot(\nabla\zeta\cdot\nabla\nabla\psi)>. \tag{5.6b}$$

We can write down $\nabla\nabla\psi$ analytically, and using our basis, average these quantities on the stream line $\psi = \psi_0$. It is now straightforward to compute the growth rate for any R or to compute critical values of R, using (3.19) and (3.20).

6. Flow in spherical geometry

Finally we move from a Cartesian geometry with flows independent of z to obtain analogous results for a spherical polar geometry with flows independent of the azimuthal coordinate. We give only a sketch. Define spherical polar coordinates (r, θ, ϕ) with corresponding unit vectors $(\hat{\mathbf{r}}, \hat{\boldsymbol{\theta}}, \hat{\boldsymbol{\phi}})$ and consider flows of the form

$$\mathbf{u} = \mathbf{u}_H(r, \theta) + W(r, \theta)\, r \sin\theta\, \hat{\boldsymbol{\phi}} \tag{6.1}$$

with

$$\mathbf{u}_H = -\frac{\partial_\theta \psi}{r^2 \sin\theta}\, \hat{\mathbf{r}} + \frac{\partial_r \psi}{r \sin\theta}\, \hat{\boldsymbol{\theta}} = \nabla\phi \times \nabla\psi = -\nabla \times \left(\frac{\psi}{r \sin\theta}\, \hat{\boldsymbol{\phi}} \right). \tag{6.2}$$

With this definition $\psi(r, \theta)$ is Stokes' stream function for the flow (see, for example, Batchelor 1967, p. 79): the flux between two stream surfaces is 2π times the difference in ψ between those surfaces. W is the azimuthal angular velocity.

6.1. The case $W(\psi)$

We consider first the case when the azimuthal angular velocity W is constant on stream surfaces, $W = W(\psi)$, analogously to section 2, and we follow this section closely. In each plane $\phi = \text{const.}$, the motion given by $\mathbf{u}_H$ is along curves of constant ψ, and we may define an angle coordinate ϑ as in (2.4). Once this is done, equations (2.5)–(2.11) carry through with z replaced by ϕ, and $\hat{\mathbf{z}}$ replaced by one of the vectors

$$\nabla\phi = (r \sin\theta)^{-1}\, \hat{\boldsymbol{\phi}}, \qquad \mathbf{e}_\phi = r \sin\theta\, \hat{\boldsymbol{\phi}} \tag{6.3}$$

as appropriate. The effects of the curved geometry only emerge when the diffusion operator is considered. In place of (2.12) we have

$$\begin{aligned}
\nabla^2 \mathbf{b} = {} & \mathbf{e}_\psi \nabla^2 b_\psi + \mathbf{e}_\vartheta \nabla^2 b_\vartheta + \mathbf{e}_\phi \nabla^2 b_\phi && \text{(6.4a)} \\
& + 2\nabla b_\psi \cdot \nabla \mathbf{e}_\psi + 2\nabla b_\vartheta \cdot \nabla \mathbf{e}_\vartheta + 2\nabla b_\phi \cdot \nabla \mathbf{e}_\phi && \text{(6.4b)} \\
& + b_\psi \nabla^2 \mathbf{e}_\psi + b_\vartheta \nabla^2 \mathbf{e}_\vartheta + b_\phi \nabla^2 \mathbf{e}_\phi. && \text{(6.4c)}
\end{aligned}$$

The important terms are those which generate b_ψ-field from b_ϑ or b_ϕ components; using $\nabla = (\nabla\psi)\partial_\psi + (\nabla\vartheta)\partial_\vartheta + (\nabla\phi)\partial_\phi$, these may be expanded as

$$\begin{aligned}
& \nabla\psi \cdot (2\nabla b_\vartheta \cdot \nabla \mathbf{e}_\vartheta + b_\vartheta \nabla^2 \mathbf{e}_\vartheta + 2\nabla b_\phi \cdot \nabla \mathbf{e}_\phi + b_\phi \nabla^2 \mathbf{e}_\phi) \\
& \quad = \quad 2\nabla\psi \cdot (\nabla\psi \cdot \nabla \mathbf{e}_\vartheta)\partial_\psi b_\vartheta + 2\nabla\psi \cdot (\nabla\vartheta \cdot \nabla \mathbf{e}_\vartheta)\partial_\vartheta b_\vartheta && \text{(6.5a,b)} \\
& \qquad + 2\nabla\psi \cdot (\nabla\phi \cdot \nabla \mathbf{e}_\vartheta)\partial_\phi b_\vartheta + (\nabla\psi \cdot \nabla^2 \mathbf{e}_\vartheta) b_\vartheta && \text{(6.5c,d)} \\
& \qquad + 2\nabla\psi \cdot (\nabla\psi \cdot \nabla \mathbf{e}_\phi)\partial_\psi b_\phi + 2\nabla\psi \cdot (\nabla\vartheta \cdot \nabla \mathbf{e}_\phi)\partial_\vartheta b_\phi && \text{(6.5e,f)} \\
& \qquad + 2\nabla\psi \cdot (\nabla\phi \cdot \nabla \mathbf{e}_\phi)\partial_\phi b_\phi + (\nabla\psi \cdot \nabla^2 \mathbf{e}_\phi) b_\phi && \text{(6.5g,h)} \\
& \quad \equiv \quad (2\lambda_{\mathrm{a}}\partial_\psi + 2\lambda_{\mathrm{b}}\partial_\vartheta + 2\lambda_{\mathrm{c}}\partial_\phi + \lambda_{\mathrm{d}}) b_\vartheta \\
& \qquad + (2\lambda_{\mathrm{e}}\partial_\psi + 2\lambda_{\mathrm{f}}\partial_\vartheta + 2\lambda_{\mathrm{g}}\partial_\phi + \lambda_{\mathrm{h}}) b_\phi.
\end{aligned}$$

We have defined eight coupling terms $\lambda_{\rm a}$–$\lambda_{\rm h}$. Most of these are unimportant; we have

$$\lambda_{\rm c} = \lambda_{\rm e} = \lambda_{\rm f} = \lambda_{\rm h} = 0, \quad \overline{\lambda}_{\rm a} = \overline{\lambda}_{\rm d} = \overline{\lambda}_{\rm g} = 0, \quad \overline{\lambda}_{\rm b} = \alpha_m. \tag{6.6}$$

Only one term can contribute to the dynamo process: $\alpha_m \equiv \overline{\lambda}_{\rm b} = <\nabla\psi \cdot (\nabla\vartheta \cdot \nabla \mathbf{e}_\vartheta)>$, and this term is the same as that in (2.17) of section 2.

The results (6.6) can be established in a variety of manners. Using formulae for the vector calculus operators in spherical polar coordinates (e.g., Batchelor 1967, p. 600), it may be confirmed that $\lambda_{\rm c}$, $\lambda_{\rm e}$, $\lambda_{\rm f}$, $\lambda_{\rm h}$ are all zero. The proofs of the remaining results follow those of section 2 closely. Equation (2.18) still holds, and it then follows that (2.20) becomes

$$2\pi <\mathbf{e}_\vartheta \cdot (*)> = \oint_{\partial S_\psi} (*) \cdot d\mathbf{r} = \int_{S_\psi} \hat{\boldsymbol{\phi}} \cdot \nabla \times (*)\, dS, \tag{6.7}$$

where again S_ψ is the interior of the curve $\psi =$ const. in any plane $\phi =$ const. However (2.19) is modified since now $qr\sin\theta = |\nabla\psi|$; consider integrating also over the angle ϕ,

$$\nabla\psi\, d\vartheta\, d\phi = \nabla\psi\, \frac{\Omega(\psi)}{q}\, ds\, d\phi = \Omega(\psi)\, r\sin\theta\, \hat{\mathbf{n}}\, ds\, d\phi = \Omega(\psi)\, \hat{\mathbf{n}}\, dS \qquad \Big(\hat{\mathbf{n}} \equiv \frac{\nabla\psi}{|\nabla\psi|}\Big), \tag{6.8}$$

where dS is the area element on the torus $\psi =$ const. in three-dimensional space. If we denote this torus by ∂T_ψ and its interior by T_ψ then we have in place of (2.21)

$$(2\pi)^2 <\nabla\psi \cdot (*)> = \Omega(\psi) \int_{\partial T_\psi} (*) \cdot \hat{\mathbf{n}}\, dS = \Omega(\psi) \int_{T_\psi} \nabla \cdot (*)\, dV. \tag{6.9}$$

The proof that $\overline{\lambda}_{\rm a} = 0$ goes through now exactly as before. For $\overline{\lambda}_{\rm d}$ (2.23) continues to hold and the first term again averages to zero using (6.9). For the second term

$$\begin{aligned} \nabla\psi \cdot (\nabla\psi \cdot \nabla \mathbf{u}_H) &= \nabla\psi \cdot (\nabla\psi \cdot \nabla(\nabla\phi \times \nabla\psi)) = \nabla\psi \cdot (\nabla\phi \times \nabla \tfrac{1}{2}|\nabla\psi|^2) \\ &= -\nabla\psi \cdot \nabla \times \Big(\frac{\frac{1}{2}|\nabla\psi|^2}{r\sin\theta}\, \hat{\boldsymbol{\phi}} \Big) \end{aligned} \tag{6.10}$$

(cf. (6.2)) and this averages to zero by (6.9). For $\overline{\lambda}_{\rm g}$ consider

$$\nabla\phi \cdot \nabla \mathbf{e}_\phi = -r^{-1}(\hat{\mathbf{r}} + \cot\theta\, \hat{\boldsymbol{\theta}}) = \nabla \times (\cot\theta\, \hat{\boldsymbol{\phi}}) \tag{6.11}$$

from (6.3), and so using (6.9) $\overline{\lambda}_{\rm g} = 0$.

Moving now into section 2.3, everything follows with minor modifications, principally replacing z by ϕ. Note that the magnetic field has a dependence as $e^{ik\phi}$; so that k becomes an azimuthal wave number, now restricted to be an integer. Equation (2.33) becomes

$$\Delta_k = |\nabla\psi|^2 \partial_\Psi^2 + \varepsilon^{1/4} 2(\nabla\vartheta \cdot \nabla\psi)\partial_\Psi \partial_\vartheta + \varepsilon^{1/2} |\nabla\vartheta|^2 \partial_\vartheta^2 - \varepsilon^{1/2} (r\sin\theta)^{-2} k^2. \tag{6.12}$$

Equation (2.42a) acquires a new term $2\lambda_{\rm g}\partial_\phi B_{\phi 0}$ but since $\overline{\lambda}_{\rm g} = 0$ this disappears on averaging in going to (2.43). The final result is that the growth rate is given exactly as in section 2.4, except that k^2 (the very last term in (2.50)) is replaced by $\beta_k k^2$ where

$$\beta_k = <(r\sin\theta)^{-2}> = <|\nabla\phi|^2>.$$

The only term affected is that representing diffusion in the azimuthal direction; the remaining equations and discussion in section 2.4 are unchanged.

6.2. The case $W(r,\theta)$

We now allow the azimuthal angular velocity W to be a general function of ψ and ϑ. We follow the procedure of section 3 and break W into mean and fluctuating components,

$$W(r,\theta) \equiv W(\psi,\vartheta) = \overline{W}(\psi) + \widetilde{W}(\psi,\vartheta). \tag{6.13}$$

We define a new coordinate ζ analogously to (3.3) (replacing z by ϕ); with this choice equation (3.5) holds in the spherical geometry, and the calculations proceed analogously to those in section 3. The two bases used are $\{\nabla\psi, \nabla\vartheta, \nabla\zeta\}$ and $\{\mathbf{f}_\psi, \mathbf{f}_\vartheta, \mathbf{e}_\phi\}$, with the vectors defined analogously to those in section 3, but replacing $\hat{\mathbf{z}}$ by $\nabla\phi$ and $\mathbf{e}_\phi$ in (3.6) and (3.8), respectively.

The diffusive coupling terms that need to be considered are

$$\begin{aligned}
&\nabla\psi\cdot(2\nabla b_\vartheta\cdot\nabla\mathbf{f}_\vartheta + b_\vartheta\nabla^2\mathbf{f}_\vartheta + 2\nabla b_\zeta\cdot\nabla\mathbf{e}_\phi + b_\zeta\nabla^2\mathbf{e}_\phi)\\
&\quad= \quad 2\nabla\psi\cdot(\nabla\psi\cdot\nabla\mathbf{f}_\vartheta)\partial_\psi b_\vartheta + 2\nabla\psi\cdot(\nabla\vartheta\cdot\nabla\mathbf{f}_\vartheta)\partial_\vartheta b_\vartheta && \text{(6.14a,b)}\\
&\qquad + 2\nabla\psi\cdot(\nabla\zeta\cdot\nabla\mathbf{f}_\vartheta)\partial_\zeta b_\vartheta + (\nabla\psi\cdot\nabla^2\mathbf{f}_\vartheta)b_\vartheta && \text{(6.14c,d)}\\
&\qquad + 2\nabla\psi\cdot(\nabla\psi\cdot\nabla\mathbf{e}_\phi)\partial_\psi b_\zeta + 2\nabla\psi\cdot(\nabla\vartheta\cdot\nabla\mathbf{e}_\phi)\partial_\vartheta b_\zeta && \text{(6.14e,f)}\\
&\qquad + 2\nabla\psi\cdot(\nabla\zeta\cdot\nabla\mathbf{e}_\phi)\partial_\zeta b_\zeta + (\nabla\psi\cdot\nabla^2\mathbf{e}_\phi)b_\zeta && \text{(6.14g,h)}\\
&\quad\equiv \quad (2\mu_{\rm a}\partial_\psi + 2\mu_{\rm b}\partial_\vartheta + 2\mu_{\rm c}\partial_\phi + \mu_{\rm d})b_\vartheta\\
&\qquad + (2\mu_{\rm e}\partial_\psi + 2\mu_{\rm f}\partial_\vartheta + 2\mu_{\rm g}\partial_\phi + \mu_{\rm h})b_\phi.
\end{aligned}$$

The properties of the coefficients $\mu_{\rm a}$–$\mu_{\rm h}$ may be summarised by

$$\mu_{\rm e} = \mu_{\rm f} = \mu_{\rm h} = 0, \quad \overline{\mu}_{\rm a} = \overline{\mu}_{\rm d} = \overline{\mu}_{\rm g} = 0, \quad \overline{\mu}_{\rm b} = \alpha_m, \quad \overline{\mu}_{\rm c} = \alpha_k \tag{6.15}$$

and we have two alpha effect terms. The first is

$$\alpha_m \equiv \overline{\mu}_{\rm b} = <\nabla\psi\cdot(\nabla\vartheta\cdot\nabla\mathbf{f}_\vartheta)>; \tag{6.16}$$

this may be simplified to

$$\alpha_m = <\nabla\psi\cdot(\nabla\vartheta\cdot\nabla\mathbf{e}_\vartheta)> \equiv \overline{\lambda}_{\rm b}, \tag{6.17}$$

which is the familar form. The second alpha effect term is

$$\alpha_k \equiv \overline{\mu}_{\rm c} = <\nabla\psi\cdot(\nabla\zeta\cdot\nabla\mathbf{f}_\vartheta)>, \tag{6.18}$$

which does not simplify very much. It can be rewritten as the two terms in (3.15) for the Cartesian case, plus an extra term arising from the spherical geometry

$$\alpha_k \equiv \overline{\mu}_{\rm c} = -<\lambda_{\rm a}\partial_\psi Z> - <\lambda_{\rm b}\partial_\vartheta Z> - \Omega^{-1}<\widetilde{W}\mathbf{e}_\phi\cdot(\nabla\phi\cdot\nabla\nabla\psi)>. \tag{6.19}$$

We now indicate why equations (6.15) hold. The vanishing of $\mu_{\rm e} \equiv \lambda_{\rm e}$, $\mu_{\rm f} \equiv \lambda_{\rm f}$ and $\mu_{\rm h} \equiv \lambda_{\rm h}$ follows from section 6.1. Now

$$\mu_{\rm a} = -\mathbf{f}_\vartheta \cdot (\nabla\psi \cdot \nabla\nabla\psi), \tag{6.20}$$

as $\mathbf{f}_\vartheta \cdot \nabla\psi = 0$. If we represent the quantity $\nabla\nabla\psi$ explicitly using a dyadic notation,

$$\begin{aligned}\nabla\nabla\psi = {} & (\partial_r^2\psi)\hat{\mathbf{r}}\hat{\mathbf{r}} + (r^{-1}\partial_r\partial_\theta\psi - r^{-2}\partial_\theta\psi)(\hat{\mathbf{r}}\hat{\boldsymbol{\theta}} + \hat{\boldsymbol{\theta}}\hat{\mathbf{r}}) \\ & + (r^{-2}\partial_\theta^2\psi + r^{-1}\partial_r\psi)\hat{\boldsymbol{\theta}}\hat{\boldsymbol{\theta}} + (r^{-1}\partial_r\psi + r^{-2}\cot\theta\,\partial_\theta\psi)\hat{\boldsymbol{\phi}}\hat{\boldsymbol{\phi}},\end{aligned} \tag{6.21}$$

we see that

$$\mu_{\rm a} = -\mathbf{e}_\vartheta \cdot (\nabla\psi \cdot \nabla\nabla\psi) = \nabla\psi \cdot (\nabla\psi \cdot \nabla\mathbf{e}_\vartheta) = \lambda_{\rm a}, \tag{6.22}$$

and so $\overline{\mu}_{\rm a} = \overline{\lambda}_{\rm a} = 0$ as in section 2. Using a similar argument

$$\mu_{\rm g} = -\mathbf{e}_\phi \cdot (\nabla\zeta \cdot \nabla\nabla\psi) = -\mathbf{e}_\phi \cdot (\nabla\phi \cdot \nabla\nabla\psi) = \nabla\psi \cdot (\nabla\phi \cdot \nabla\mathbf{e}_\phi) = \lambda_{\rm g}, \tag{6.23}$$

and so $\overline{\mu}_{\rm g} = \overline{\lambda}_{\rm g} = 0$ as before. For $\mu_{\rm d}$,

$$\mu_{\rm d} = \nabla\psi \cdot \nabla^2(\mathbf{e}_\vartheta + \mathbf{e}_\phi\,\widetilde{W}/\Omega) = \nabla\psi \cdot \nabla^2\mathbf{e}_\vartheta = \lambda_{\rm d}, \tag{6.24}$$

and again averages to zero. When this is done, we finally obtain the growth rate as in section 3.2; all equations and discussion in that section hold for the spherical polar case outlined here.

7. Discussion

We have analysed generalised Ponomarenko dynamos in the limit of large magnetic Reynolds number in both Cartesian and spherical geometry. We have obtained two types of alpha effect. The first alpha effect, which we denote α_m, is very robust and is the same in all situations. It depends only on the shape of stream lines in a horizontal plane for Cartesian geometry, or a meridional plane for spherical geometry. The second alpha effect, denoted α_k, arises when the vertical velocity for Cartesian geometry, or the azimuthal angular velocity for spherical geometry, is not constant on stream lines. We have also identified diffusive effects, and given formulae for growth rates of magnetic field modes over a wide range of scales. These are confirmed by full-scale numerical simulations in Cartesian geometry.

Our analysis is based on a number of assumptions. One is the key condition that $m\Omega'' + k\overline{W}'' \neq 0$ on the stream surface, or equivalently that $\Omega''/\Omega' - \overline{W}''/\overline{W}' \neq 0$. In our study the magnetic field mode must experience *some* differential rotation in the neighbourhood of the resonant surface. While it vanishes at leading order because of the resonance condition $m\Omega' + k\overline{W}' = 0$, it must be present at higher order to localise the mode. In the non-generic cases where it fails to (for example when all stream lines are closed), dynamo action will still occur but the present asymptotic framework requires modification; this is considered for the case of circular stream lines by Ruzmaikin *et al.* (1988).

Thinking of the Cartesian case for simplicity, another important assumption is that the horizontal velocity $\mathbf{u}_H$ should nowhere vanish on the stream surface. However direct numerical simulations of dynamos in a plane layer show that often magnetic modes are precisely associated with such stagnation points of $\mathbf{u}_H$ and the separatrices joining them (see Plunian *et al.* 1999, Ponty *et al.* 2000). It would be interesting to obtain formulae of some generality for dynamo action in this case, building on the work of Childress (1979), Soward (1987), Childress & Soward (1989) and Soward & Childress (1990).

In fact one can think of our study as being the one of a number of possible asymptotic calculations of dynamo growth rates at high R in generic steady fluid flows independent of one coordinate, say z, in an infinite fluid. If one writes down a general $\mathbf{u}_H(x, y)$ one may have isolated points where $\mathbf{u}_H = 0$, that are either elliptic or hyperbolic with separatrices. Elsewhere the stream lines will either be closed or form channels. We have studied in this paper the first case, of general closed stream lines for a general $W(x, y)$. The results could be adapted to obtain dynamo action in the second case, of channel flows, provided the individual stream lines are periodic and so averaging methods may be applied. This leaves two further cases: third, dynamo action with the fields localised around hyperbolic points joined by separatrices. Finally, there is dynamo action in channel flows in which an individual stream line is aperiodic, and approaches arbitrarily close to hyperbolic stagnation points. These four cases cover all the generic stream surfaces in a steady flow independent of one coordinate, and parallel the sequence of studies of Childress and Soward listed above, in which particular velocity fields, based on ABC flows, are considered and alpha effects computed.

If the flow is allowed to depend on a third spatial coordinate or time, then the additional, difficult element of chaotic stretching is introduced into the flow, and other techniques are required (see Childress & Gilbert 1995). Finally the study of kinematic dynamo action presented here may form the basis of future studies of non-linear dynamo equilibration and extensions of Bassom & Gilbert (1997).

Acknowledgements

We are grateful to Prof. C.A. Jones, Dr. G. Sarson, Prof. A.M. Soward, Dr. A. Tilgner and Prof. K. Zhang for helpful conversations, and to Dr. D.D. Sokoloff and an anonymous referee for helpful comments. We should like to thank Dr. A. Alemany, Dr. P. Marty and Dr. F. Plunian for kindly sending us their numerical results that were used for the comparison in figure 9. The work of YP is supported by a research grant from the Leverhulme Trust. The numerical calculations were performed using the computing facilities of the laboratory Cassini, Observatoire de Nice (France), provided by the program "Simulations Interactives et Visualisation en Astronomie et Mécanique (SIVAM)" and the computing facilities of the parallel computer Ceres at the University of Exeter.

References

Abramowitz, M. & Stegun, I.A. 1965 *Handbook of Mathematical Functions.* Dover.

Bassom, A.P. & Gilbert, A.D. 1997 Nonlinear equilibration of a dynamo in a smooth helical flow. *J. Fluid Mech.* **343**, 375-406.

Bassom, A.P. & Gilbert, A.D. 2000 The relaxation of vorticity fluctuations in approximately elliptical stream lines. *Proc. R. Soc. Lond. A* **456**, 295–314.

Basu, A. 1997 Screw dynamo and the generation of nonaxisymmetric magnetic fields. *Phys. Rev. E.* **56**, 2869–2874.

Batchelor, G.K. 1967 *An Introduction to Fluid Mechanics.* Cambridge University Press.

Braginsky, S.I. 1964a Self-excitation of a magnetic field during the motion of a highly conducting fluid. *Zh. Exp. Teor. Fiz. SSSR* **47**, 1084–1098. (English transl.: *Sov. Phys. JETP* **20**, 726–735 (1965).)

Braginsky, S.I. 1964b Theory of the hydromagnetic dynamo. *Zh. Exp. Teor. Fiz. SSSR* **47**, 2178–2193. (English transl.: *Sov. Phys. JETP* **20**, 1462–1471 (1965).)

Childress, S. 1979 Alpha-effect in flux ropes and sheets. *Phys. Earth Planet. Int.* **20**, 172–180.

Childress, S. & Gilbert, A.D. 1995 *Stretch, twist, fold: the fast dynamo.* Lecture Notes in Physics: Monographs, vol. 37. Springer–Verlag.

Childress, S. & Soward, A. M. 1989 Scalar transport and alpha-effect for a familly of cat's-eyes flows. *J. Fluid Mech.* **205**, 99–133.

Dudley, M.L. & James, R.W. 1989 Time-dependent kinematic dynamos with stationary flows *Proc. R. Soc. Lond. A* **425**, 407–429.

Gailitis, A.K. 1993 Experimental aspects of a laboratory scale liquid sodium dynamo model. In: *Solar and Planetary Dynamos* (ed. M.R.E. Proctor, P.C. Matthews, A.M. Rucklidge), pp. 91–98. Cambridge University Press.

Gailitis, A.K. & Freiberg, Ya.G. 1980 Non-uniform model of a helical dynamo. *Magn. Gidrodin.*, no. 1, 15–19. (English transl.: *Magnetohydrodynam.* **16**, 11–15.)

Gailitis, A.K., Karasev, B.G., Kirillov, I.R., Lielausis, O.A., Luzhanskij, S.M., Ogorodnikov, A.P. & Preslitskij, G.V. 1987 *Liquid metal MHD dynamo model.* Publ. by Physics Institute, Latvian SSR Academy of Sciences.

Gailitis, A.K., Lielausis, O.A., Dement'ev, S., Platacis, E., Cifersons, A., Gerbeth, G., Gundrum, T., Stefani, F., Christen, M., Hänel, H., & Will, G. 1999 Detection of a flow induced magnetic field eigenmode in the Riga dynamo facility. *Phys. Rev. Lett.*, submitted.

Gilbert, A.D. 1988 Fast dynamo action in the Ponomarenko dynamo. *Geophys. Astrophys. Fluid Dyn.* **44**, 241–258.

Lortz, D. 1968 Exact solutions of the hydromagnetic dynamo problem. *Plasma Phys.* **10**, 967–972.

Plunian, F., Marty, P. & Alemany, A. 1999 Kinematic dynamo action in a network of screw motions; application to the core of a fast breeder reactor. *J. Fluid Mech.* **382**, 137–154.

Ponomarenko, Yu.B. 1973 On the theory of hydromagnetic dynamos. *Zh. Prikl. Mech. Tech. Fiz. (USSR)* **6**, 47–51.

Ponty, Y., Gilbert, A.D. & Soward, A.M. 2000 Kinematic dynamo action in flows driven by shear and convection. *J. Fluid Mech.*, submitted.

Rhines, P.B. & Young, W.R. 1983 How rapidly is a passive scalar mixed within closed streamlines? *J. Fluid Mech.* **133**, 133–145.

Roberts, G.O. 1970 Spatially periodic dynamos. *Phil. Trans. R. Soc. Lond. A* **266**, 535–558.

Roberts, P.H. 1987 Dynamo theory. In *Irreversible Phenomena and Dynamical Systems Analysis in Geosciences* (ed. C. Nicolis & G. Nicolis), pp. 73–133. D. Reidel.

Ruzmaikin, A.A., Sokoloff, D.D. & Shukurov, A.M. 1988 A hydromagnetic screw dynamo. *J. Fluid Mech.* **197**, 39–56.

Shukurov, A.M. & Sokoloff, D.D. 1993 Evolution of magnetic fields in a swirling jet. In: *Solar and Planetary Dynamos* (ed. M.R.E. Proctor, P.C. Matthews, A.M. Rucklidge), pp. 271–274. Cambridge University Press.

Solovyev, A.A. 1985 Excitation of magnetic field by the axisymmetric motion of a conducting fluid. *Izv. Akad. Nauk USSR, Fiz. Zemli*, no. 4, 101–103.

Solovyev, A.A. 1987 Magnetic field excitation by conducting fluid flow at high magnetic Reynolds numbers. *Izv. Akad. Nauk USSR, Fiz. Zemli*, no. 5, 77–80.

Soward, A.M. 1987 Fast dynamo action in a steady flow. *J. Fluid Mech.* **180**, 267–295.

Soward, A.M. 1990 A unified approach to a class of slow dynamos. *Geophys. Astrophys. Fluid Dyn.* **53**, 81–107.

Soward, A.M., Childress, S. 1990 Large magnetic Reynolds number dynamo action in spatially periodic flow with mean motion. *Phil. Trans. R. Soc. Lond. A* **331**, 649–733.

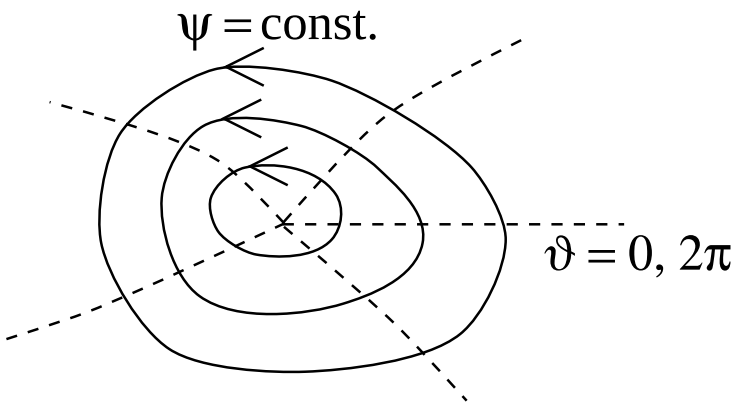

FIGURE 1

Figure 1: A schematic depiction of coordinates (ψ, ϑ) in the (x, y)-plane.

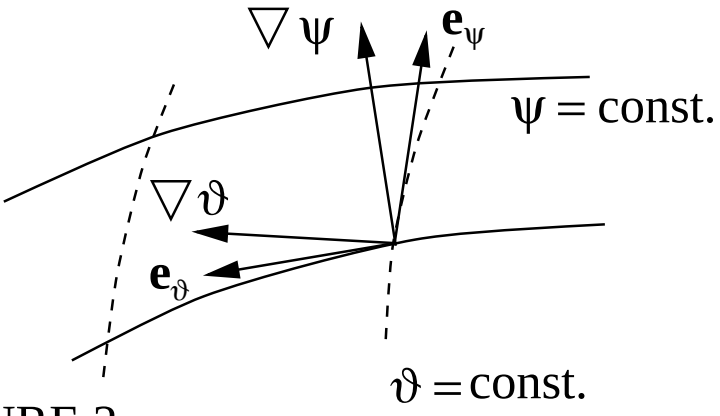

FIGURE 2

Figure 2: The vectors $\nabla\psi$, $\nabla\vartheta$, $\mathbf{e}_\psi$ and $\mathbf{e}_\vartheta$.

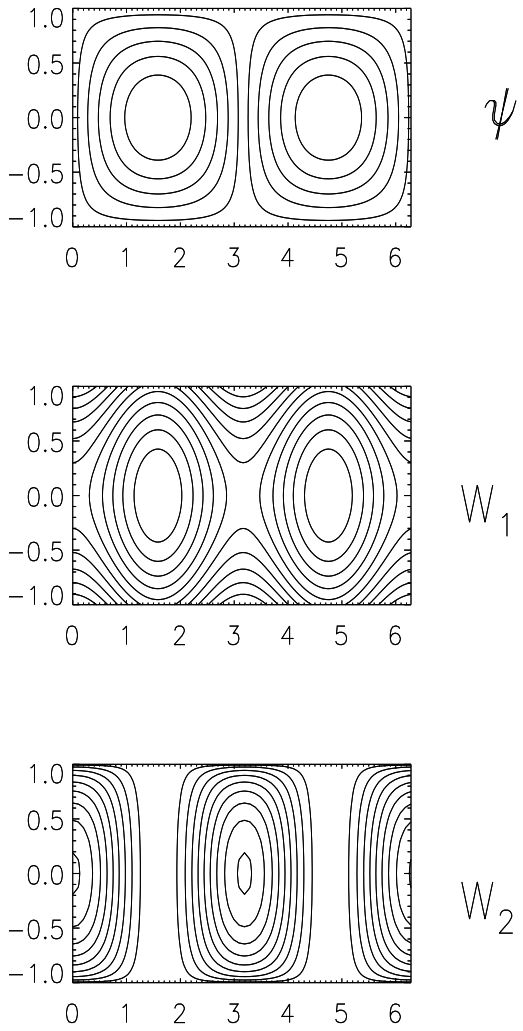

Figure 3: Flows used in numerical simulations. Contour plots are shown of (a) the stream function ψ, and the vertical velocities (b) W_1 and (c) W_2.

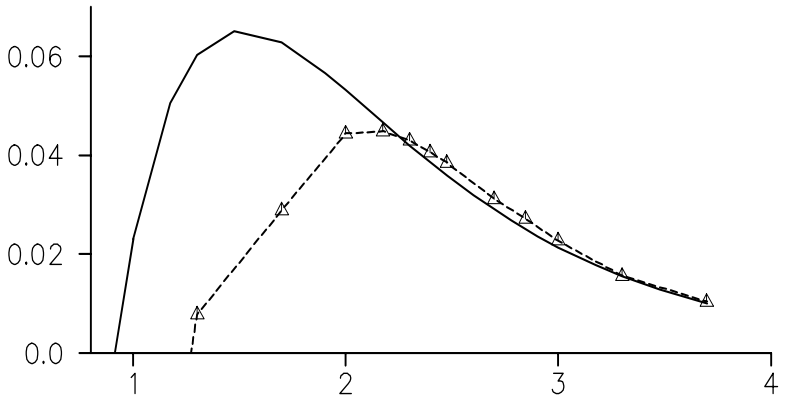

Figure 4: Growth rate p plotted against $\log_{10} R$ for the flow given by ψ, W_1, with $k = 0.7$, $m = 1$. The numerical results are shown by markers joined by a dotted line; the asymptotic results are shown by a solid line.

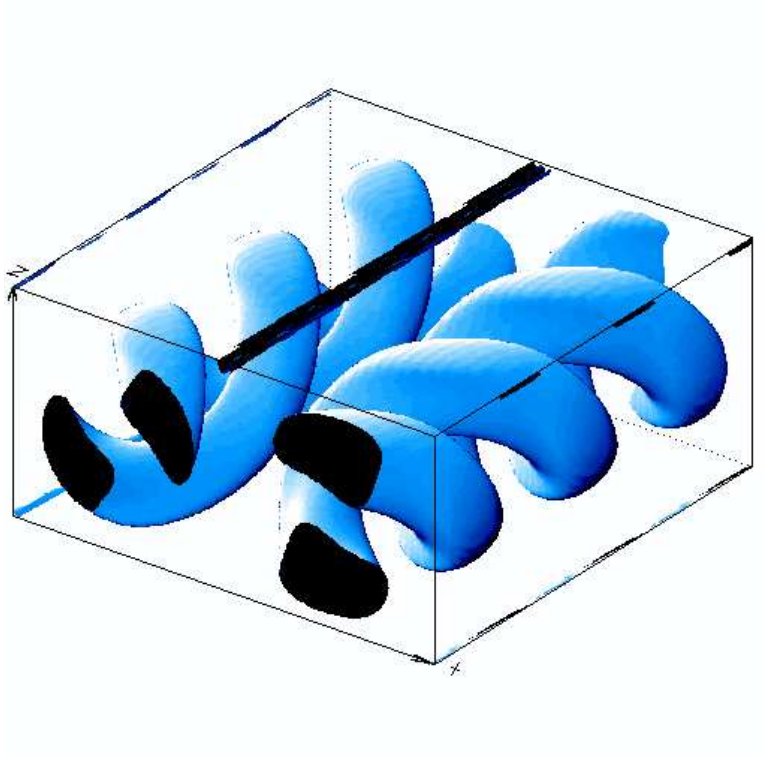

Figure 5: Growing magnetic field for the flow given by ψ, W_1, with $k = 0.7$, $m = 1$ and $R = 500$. An isosurface of constant magnetic field magnitude is shown in three dimensions.

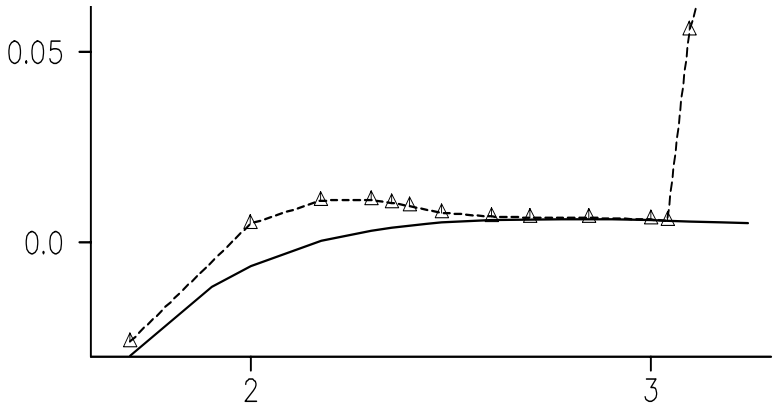

Figure 6: Growth rate p plotted against $\log_{10} R$ for the flow given by ψ, W_2, with $k = 1.5$, $m = 1$. The numerical results are shown by markers joined by a dotted line; the asymptotic results are shown by a solid line.

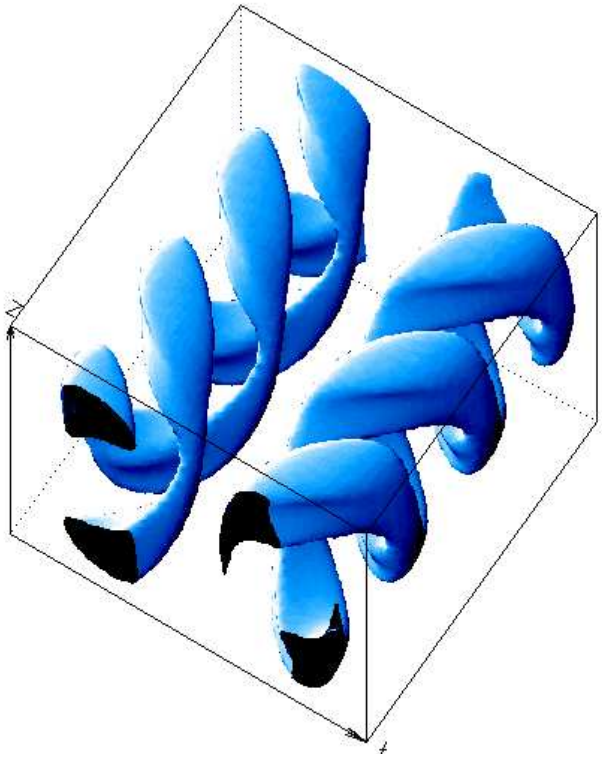

Figure 7: Growing magnetic field for the flow given by ψ, W_2, with $k = 1.5$, $m = 1$ and $R = 500$. An isosurface of constant magnetic field magnitude is shown in three dimensions.

Figure 8: Growing magnetic field for the flow given by ψ, W_2, with $k = 1.5$, $m = 1$ and $R = 2000$. An isosurface of constant magnetic field magnitude is shown in three dimensions.

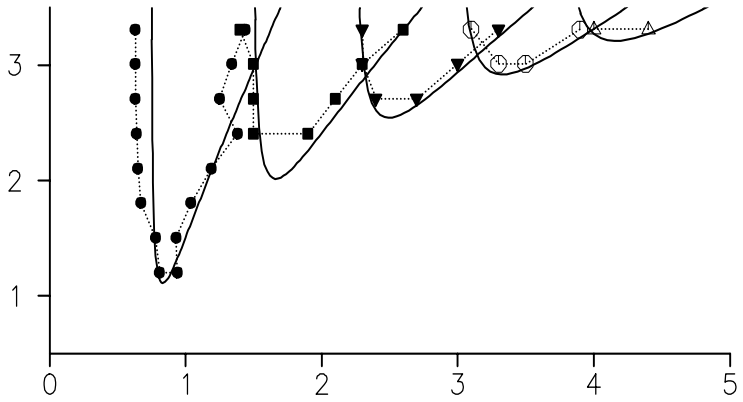

Figure 9: Comparison between the results of Plunian *et al.* (1999) and the asymptotic theory. Theoretical curves (solid) of $\log_{10} R_c$ are plotted as a function of k for $m = 1$, 2, 3, 4 and 5, reading the curves from left to right. Numerical results of Plunian *et al.* (1999) are shown by markers joined by dotted lines with $m = 1$ (solid circles), 2 (solid squares), 3 (solid triangles), 4 (open circles) and 5 (open triangles).